

XLRS-Bench: Could Your Multimodal LLMs Understand Extremely Large Ultra-High-Resolution Remote Sensing Imagery?

Fengxiang Wang¹, Hongzhen Wang², Mingshuo Chen³, Di Wang^{4,5}, Yulin Wang²,
 Zonghao Guo², Qiang Ma², Long Lan¹, Wenjing Yang^{1*}, Jing Zhang^{4,6}, Zhiyuan Liu², Maosong Sun²
¹ College of Computer Science and Technology, National University of Defense Technology, China
² Tsinghua University, China ³ Beijing University of Posts and Telecommunications, China
⁴ School of Computer Science, Wuhan University, China ⁵ Zhongguancun Academy, China
⁶ School of Artificial Intelligence, Wuhan University, China

<https://xlrs-bench.github.io/>

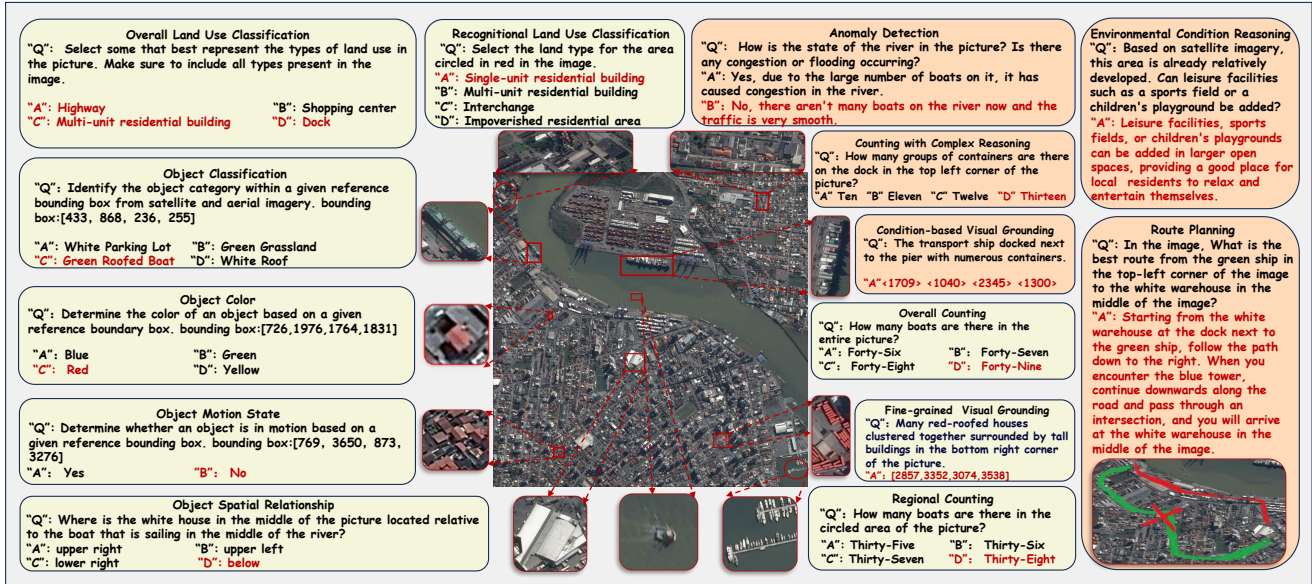


Figure 1. A typical example from our XLRS-Bench. XLRS-Bench focuses on extremely large ultra-high-resolution RS imagery, integrating over 10 multimodal vision-language perception and reasoning tasks within the same image.

Abstract

The astonishing breakthrough of multimodal large language models (MLLMs) has necessitated new benchmarks to quantitatively assess their capabilities, reveal their limitations, and indicate future research directions. However, this is challenging in the context of remote sensing (RS), since the imagery features ultra-high resolution that incorporates extremely complex semantic relationships. Existing benchmarks usually adopt notably smaller image sizes than

real-world RS scenarios, suffer from limited annotation quality, and consider insufficient dimensions of evaluation. To address these issues, we present XLRS-Bench: a comprehensive benchmark for evaluating the perception and reasoning capabilities of MLLMs in ultra-high-resolution RS scenarios. XLRS-Bench boasts the largest average image size (8500×8500) observed thus far, with all evaluation samples meticulously annotated manually, assisted by a novel semi-automatic captioner on ultra-high-resolution RS images. On top of the XLRS-Bench, 16 sub-tasks are defined to evaluate MLLMs' 10 kinds of perceptual capa-

*Corresponding authors

bilities and 6 kinds of reasoning capabilities, with a primary emphasis on advanced cognitive processes that facilitate real-world decision-making and the capture of spatiotemporal changes. The results of both general and RS-focused MLLMs on XLRs-Bench indicate that further efforts are needed for real-world RS applications. We have open-sourced XLRs-Bench to support further research in developing more powerful MLLMs for remote sensing.

1. Introduction

Recent advancements in multimodal large language models (MLLMs) [2, 44, 55, 58, 80] have significantly enhanced visual understanding and reasoning. As real-world applications require more detailed visual processing, many MLLMs [16, 29, 32, 72, 76] have been developed to improve understanding of high-resolution images. To fully assess and leverage their potential, benchmarking is essential, leading to the creation of various related datasets [5, 12, 13, 25, 34, 56, 67, 77].

Remote sensing (RS) images have become essential for monitoring and understanding human environments, driving advancements in applications like precision agriculture [75], urban planning [81], and disaster assessment [11]. As such, assessing the performance of MLLMs in this field is crucial. However, the high resolution and complex semantic relationships in RS imagery make evaluating MLLMs in real-world remote sensing contexts particularly challenging. While recent studies [28, 41, 74] have proposed benchmarks and metrics to assess MLLM performance in RS, these efforts remain limited in three key areas:

Image Size. Real ultra-high resolution RS images often capture scenes at the least city-level or above with large size (e.g., $10,000 \times 10,000$). However, benchmarks like VRS-Bench [28] merely utilize 512×512 image slices to evaluate the performance of MLLMs on cross-modal perception and understanding (like visual question answering (VQA), image captioning and visual grounding), which fails to provide a comprehensive assessment of the models’ capabilities to capture long-range spatial-semantic relationships.

Human Annotation. The prohibitive labor costs associated with comprehensive manual annotation significantly limit the scalability of existing RS multimodal benchmarks, such as LHRS-Bench [41] (only 108 RS images paired with 690 QA pairs). In response, GPT-based annotators have become widely employed to automate data construction for both training and evaluating MLLMs, thus generating substantial data volumes. Following this trend, larger-scale RS benchmarks have been created [28]. However, the absence of stringent manual calibration in automated annotation processes may lead to hallucinations and errors, compromising the quality of the data. Additionally, empirical evidence [77] indicates that benchmarks annotated

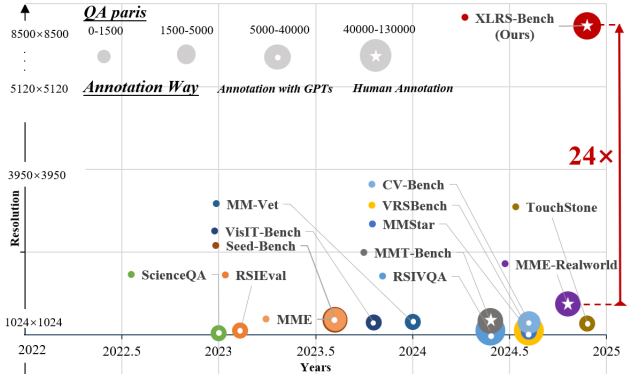


Figure 2. Advantages of XLRs-Bench: XLRs-Bench boasts an average image size that is 24 times larger than existing datasets.

by MLLMs, such as GPT-4V, often incorporate linguistic biases, which may inadvertently boost the performance of corresponding models on these benchmarks, despite attempting to manually adjust content biases.

Evaluation Dimension. Existing RS benchmarks [28, 41, 74] primarily concentrate on basic perceptual capabilities such as attribute recognition, semantic discrimination, and spatial localization. However, existing benchmarks fail to fully assess MLLMs’ interactive perception and complex reasoning, which are crucial for tasks like visual grounding, path planning, and intent inference.

To address these challenges, we introduce XLRs-Bench, a benchmark designed to assess the perception and reasoning capabilities of MLLMs on ultra-high-resolution RS scenarios. We first collected 1,400 real-world ultra-high-resolution RS images with large sizes ($8,500 \times 8,500$ pixels on average). Among them, 530 images come from detection datasets (e.g., DOTA-v2 [65]) and 870 images are from segmentation datasets (e.g., MiniFrance [6]). Then, 45 experts are involved in hand-crafted annotation and cross-verification for 16 sub-tasks. The annotations are presented as three vision-language formats including VQA, captioning and visual grounding. Specifically, we implemented a semi-automated pipeline for image captioning, by leveraging GPT-4o for pre-annotation and human for verification. We additionally invite 10 specialists in the field of MLLM for further quality control. Finally, XLRs-Bench incorporates 45,942 annotations covering 10 ability indicators for perception and 6 for reasoning, comprising 32,389 VQA pairs, 12,619 visual grounding instances, and 934 detailed captions, as shown in Fig. 1. Based on XLRs-Bench, we evaluated a series of general MLLMs and an RS-specific MLLM and conducted an in-depth analysis. As shown in Fig. 2, the key advantages of XLRs-Bench over existing benchmarks include:

- **Ultra-high Resolution.** XLRs-Bench features the largest image sizes available, $10 \sim 20 \times$ than that of existing datasets, with 840 images out of all images at a resolu-

tion of $10,000 \times 10,000$ pixels.

- **High-quality Annotation.** All the annotations are human involved and manually verified through iterations, resulting in a high-quality benchmark for evaluating MLLMs on real ultra-high-resolution RS scenarios.
- **Comprehensive Evaluation Dimensions:** XLRS-Bench covers 10 perception indicators and 6 reasoning dimensions to assess MLLMs’ capabilities, encompassing 16 sub-tasks with a total of 45,942 questions. Especially, XLRS-Bench includes complex reasoning tasks to explore MLLMs’ potential in conducting planning and change detection in long spatial-temporal RS scenarios.

In summary, our main contributions are as follows:

- We establish XLRS-Bench, a new benchmark for assessing the perception and reasoning capabilities of MLLMs across 16 sub-tasks in ultra-high-resolution RS scenarios.
- We develop a semi-automated pipeline to expand detailed captions, showcasing the potential of the scalability across various RS tasks.
- We evaluate prominent MLLMs across computer vision and RS fields on XLRS-Bench, providing insights into future directions for understanding real RS scenarios.

2. Related Work

General Multimodal Benchmark. Large-scale vision-language models (VLMs) have demonstrated great potential in multimodal tasks like complex scene understanding and visual sentiment analysis. Recently, multimodal evaluation datasets have been developed to assess the capabilities of these models quantitatively. However, previous benchmarks mainly focused on specific domains and assessed models on one or a few tasks (*e.g.*, captioning [1, 8, 68] or VQA [15, 17, 22, 38, 52, 79]). The evaluation for large-scale VLMs requires more comprehensive benchmarks. Therefore, MME [12] offers a benchmark spanning 14 perceptual and cognitive tasks, and MMBench [34] includes over 3,000 questions across 20 skill dimensions, like object localization and social reasoning. Seed-Bench [25] expands the sample size with 19,000 questions, and MMT-Bench [67] incorporates real-world data from areas like autonomous driving and embedded AI. MME-Realworld [77], extending to five real-world scenarios, provides the highest resolution natural scene benchmark so far, with images at $2,000 \times 1,500$. However, these general-purpose benchmarks have two main limitations: limited data and text annotations for RS scenarios, and smaller image sizes compared to real RS data. Even MME-Realworld, with the most RS data, includes only three types of QA pairs that are related to RS scenarios. Furthermore, its average resolution of $2,000 \times 1,500$ is still far below the required of real RS tasks (*e.g.*, HRSCD [10] at $10,000 \times 10,000$ for RS segmentation).

Remote Sensing Multimodal Benchmark. With the recent advancements of large multimodal models in gen-

eral domains, the RS field has also experienced rapid growth on MLLMs [23, 41]. This has led to the creations of relevant evaluation benchmarks. RSIEval [20] offers 100 human-annotated captions and 936 visual question-answer pairs, mainly for image captioning and VQA tasks. LHRS-Bench [41] provides 108 images and 690 questions, with VQA questions spanning five dimensions. VLEO-BENCH [39] covers scenarios such as urban monitoring, disaster relief, land use, and conservation, evaluating VLMs in scene understanding, localization, counting, and change detection tasks. What’s more, RSSA [45] introduces a benchmark focused on hallucination, while FIT-RSRC [37] targets understanding object relationships in RS scenes. VRSBench [28] includes 29,614 images with paired descriptions, 52,472 object references, and 123,221 question-answer pairs. Nevertheless, these benchmarks have two main limitations. First, they lack a diverse range of sub-tasks, resulting in less objective and comprehensive evaluations. Second, their image sizes are typically limited to 512×512 , which is far smaller than the requirements of real RS tasks (*e.g.*, DOTA [65] images reach $7,000 \times 4,000$ for detection tasks, HRSCD [10] images reach $10,000 \times 10,000$ for segmentation), hindering the evaluation of MLLMs for long-range spatial-semantic cognition in real-world RS scenarios.

Multimodal Large Language Model. Leveraging advanced LLMs like GPTs [44] and LLaMA [58], MLLMs have shown impressive capabilities [59, 60]. Proprietary models such as Gemini [55] and GPT-4o [44] exhibit strong understanding and reasoning skills, while open-source models, including Qwen-VL [2], InternLM-XComposer [72], MiniCPM [19], LLaVA [31] and MiniGPT-4 [80], also demonstrate notable performance. Since not specifically optimized for high-resolution tasks, these models only support image resolutions from 2K to 4K. Recently, several MLLMs have addressed low-resolution constraints to enable high-resolution processing. For example, LLaVA-Next [32] divides high-resolution images into patches, encodes each patch independently, and then links the patch tokens with the global image tokens. Furthermore, models such as Monkey [30] and LLaVA-UHD [16] compress these patches to avoid redundant tokens. Alternatively, Mini-Gemini [29] uses a dual encoder—one for high-resolution images and another for low-resolution embeddings, while Cambrian [57] uses learnable latent queries to interact with multiple visual features, and SHiME [76] compresses local patches twice, preserving global features. In the RS field [21, 24, 61, 62], MLLMs have advanced as well. Geochat [23], based on LLaVA-1.5 [58], enables multi-task dialogues with RS images. LHRS-Bot [41] enhances image understanding through a multi-level vision-language alignment strategy and curriculum learning, and EarthGPT [74] unifies multisensor interpretation tasks for

general RS understanding.

Despite these advancements, both RS and general-domain MLLMs face challenges. General MLLMs, while focused on high-resolution processing, lack rigorous testing on larger-size benchmarks in real-world RS scenarios. Meanwhile, RS models have only been tested on benchmarks with small images (*e.g.*, 512×512). In contrast, our XLRs-Bench provides a rigorous test bed to assess models’ perception and reasoning capabilities on large-size images from real RS environments.

3. XLRs-Bench

XLRs-Bench stands out from existing multimodal understanding benchmarks with four key features: i) the largest average image size of $8,500 \times 8,500$, featuring extensive $10,000 \times 10,000$ imagery; ii) 16 sub-tasks designed to evaluate MLLMs’ capabilities in ultra-high-resolution RS scenes; iii) strict quality control to ensure sample accuracy and validity; iv) bilingual support for evaluating VLM performance in both English and Chinese. Further details on the construction of XLRs-Bench are provided below.

3.1. Evaluation Dimensions

Humans have exceptional perception and reasoning abilities that are foundational to complex cognition. Perception gathers sensory input, while reasoning draws conclusions. Together, these abilities enable tasks like object recognition, problem-solving, and decision-making. To achieve true artificial general intelligence in the real ultra large-scale RS scenarios, MLLMs must also exhibit robust perception and reasoning capabilities. We therefore classify perception and reasoning as primary (**L-1**) abilities, further refined into 11 **L-2** and 16 **L-3** capability dimensions. Figure 3 illustrates this classification, whose detailed explanations are presented in the following text.

3.1.1. Perception

We employ two typical tasks: image captioning and VQA, to measure the L-1 perception ability. To assess the capabilities in capturing fine-grained information for large-size ultra-high-resolution RS scenes, at the L-2 level, we additionally define 6 evaluation aspects, which are further divided into 10 more refined indicators in L-3 grade. Next, we separately introduce the L-2 capabilities, with the L-3 tasks are also presented.

- **Image Captioning.** In this task, we go beyond simple single-sentence captioning tasks to *Detailed Image Captioning*, as large-size ultra-high-resolution RS images contain abundant details.
- **Scene Classification.** Scene Classification is evaluated through two L-3 sub-tasks: *Overall Land Use Classification* and *Regional Land Use Classification*. The former focuses on global image information with multiple-choice

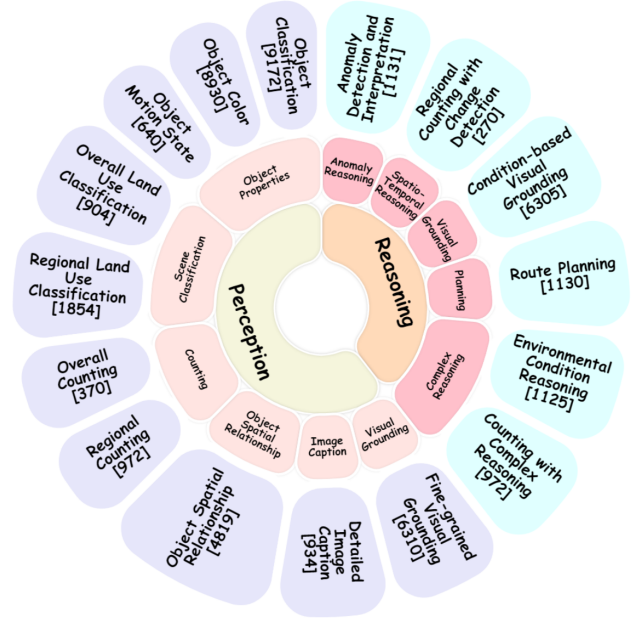


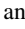










































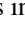





Figure 3. XLRs-Bench evaluates the perception and reasoning capabilities of MLLMs across three levels and 16 sub-tasks.

questions, while the latter examines detailed scene understanding in localized areas using single-choice questions.

- **Counting.** This capability contains two L-3 dimensions: *Overall Counting* and *Regional Counting*. Overall Counting requires comprehensive object recognition for the whole image, which is challenging even for humans. Regional Counting narrows the focus to smaller areas.
- **Object Spatial Relationship.** This dimension requires the model to identify two specified objects and determine their spatial relationship, demanding advanced spatial perception and understanding ability.
- **Object Properties.** Object understanding is assessed across three L-3 dimensions: *Object Classification*, *Object Color*, and *Object Motion State*. We exclude properties like shape and size [28], as they fall under Object Classification. Here, we conduct a separate evaluation of Object Color, since it differs significantly from attributes like shape and size. Object Motion State is especially relevant, as it tests reasoning through context clues, such as inferring a ship’s movement from its wake.
- **Visual Grounding.** This dimension tests the model’s ability to precisely locate objects. We assess *Fine-grained Visual Grounding*, which is essential in RS, where the model is required to detect small object types in large-scale high-resolution scenarios. Notably, some objects in these large-size images may be as small as 5-10 pixels, which presents a challenge for current MLLMs that primarily support 2K resolution, compressing such objects to just 1-2 pixels.

Table 1. Comparison between existing vision-language benchmarks and our benchmark. ,  and  separately represent the annotations are machine generated, manually written and semi-automated, *i.e.*, machine generation followed by human verification.

Dataset	Average Resolution	Remote Sensing	Detailed Caption		Visual Grounding		VQA	
			Volume	Average Length	Volume	Annotation Method	Volume	Annotation Method
MMStar [7]	512×375	N	-	-	-		1,500	
ScienceQA [50]	378×249	N	-	-	-		21,000	
MM-Vet [69]	1,200×675	N	-	-	-		218	
Seed-Bench [25]	1,024×931	N	-	-	-		19,242	
MMT-Bench [67]	2,365×377	N	-	-	-		32,325	
TouchStone [3]	897×803	N	-	-	-		908	
VisIT-Bench [5]	765×1,024	N	-	-	-		1,159	
BLINK [13]	620×1,024	N	-	-	-		3,807	
CV-Bench [56]	1,024×768	N	-	-	-		2,638	
MME [12]	1,161×840	N	-	-	-		2,374	
MMBench [34]	512×270	N	-	-	-		3,217	
MME-Realworld [77]	2,000×1,500	N	-	-	-		29,429	
UCM-Captions [47]	250×250	Y	10,500	12	-		-	
RSICD [36]	500×500	Y	54,605	12	-		-	
RSICap [20]	512×512	Y	2,585	60	-		-	
RSVG [53]	800×800	Y	-	-	7,933		-	
DIOR-RSVG [70]	800×800	Y	-	-	38,320		-	
RRSIS-D [33]	800×800	Y	-	-	17,402		-	
RSVQA-HR [35]	1,024×1,024	Y	-	-	-		1,066,316	
RSIVQA [78]	512×512	Y	-	-	-		111,134	
RSIEval [20]	512×512	Y	-	-	-		933	
VRSBench [28]	512×512	Y	29,614	52	52,472		123,231	
XLRS-Bench	8,500×8,500	Y	934	379	12,619		32,389	

3.1.2. Reasoning

Unlike previous assessments of simple reasoning [28], we would like to evaluate the model’s ability to perform Complex Reasoning based on rich visual information in ultra-high-resolution RS scenarios. We designed challenging 5 L-2 dimensions and 6 L-3 dimensions to test reasoning in realistic ultra-high-resolution RS scenarios:

- **Complex Reasoning.** It is divided into two L-3 dimensions, *Environmental Condition Reasoning* and *Counting with Complex Reasoning*. The former dimension leverages the comprehension information in ultra-high-resolution images, requiring the model to make contextual inferences. *Counting with Complex Reasoning* requires not only perception-based counting but also the ability to perform complex reasoning.
- **Anomaly Reasoning.** The model is expected to detect anomalies and predict potential risks using contextual clues, named *Anomaly Detection and Interpretation*. For instance, in a town near a mountain, the model should identify exposed forest land and, considering climate conditions, predict possible landslide risks.
- **Planning.** Beyond reasoning, the model should plan a route based on provided conditions, named *Route Planning* (L-3 ability). Given a starting point described in natural language, the model must locate it accurately on the image and select an optimal route based on criteria like shortest distance or minimal intersections.
- **Visual Grounding.** We also include conditional grounding to evaluate reasoning-based localization abilities, named *Condition-based Visual Grounding* (L-3 ability). Here, the model locates objects by inferring based on

complex conditions in the image.

- **Spatiotemporal Reasoning.** The *Regional Counting with Change Detection* is unique in the RS field, as it evaluates changes in the number of objects between two temporal images of the same location.

3.2. Data Collection and Quality Control

Data Source To create a benchmark with diverse evaluation dimensions, we collected large-size high-resolution RS images rich in visual details, in order to design varied and challenging assessment tasks. Specifically, we compiled 1,400 images from realistic RS scenarios for different downstream tasks, selecting them rigorously based on diversity and quality. For detection tasks, we sourced 270 images at 4,096×4,096 and 210 images at 7,360×4,912 from DOTA-v2 [65], and added 50 images at a size of 3,744×5,616 from the ITCVD [66] dataset. For segmentation tasks, we used 457 images at 10,000×10,000 resolution from MiniFrance [6], 13 images at 11,500×7,500 from Toronto [49], and 30 images at 6,000×6,000 from Potsdam [48]. Additionally, for change detection tasks, we included 185 pairs (370 images) at 10,000×10,000 resolution from the HRSCD [10] dataset. Each image underwent multi-round cross-validation by annotators to ensure a rich, diverse selection of large-size and ultra-high-resolution samples. To be noticed, our dataset includes 840 images at 10,000×10,000 pixels—a significant milestone in benchmark works. To the best of our knowledge, this is the first large-scale evaluation using 10,000×10,000 images. Although challenging for human evaluation, we believe it is an essential step toward realistic RS applications.

Visual Question Answering In XLRs-Bench, we compile visual language question-answer pairs in a multiple-choice format for each L-3 capability, excluding grounding and captioning dimensions. Each pair $(P_i = (Q_i, C_i, I_i, T_i))$ includes: Q_i (the question), C_i (a set of n options, $2 \leq n \leq 4$), I_i (the relevant image), and T_i (the correct answer). It is important to note that research indicates GPT-based tools can introduce bias in benchmarks, favoring similar models and compromising their rigor and real-world assessment capacity [77]. To address this, trained annotators expand the question set through human-only annotation, avoiding the assistance of GPTs. To minimize design bias, we implemented cross-validation and formed an external review team. Specifically, three annotation groups, each with 15 members, cross-validated each other’s work, while a review team of 10 experts with MLLM experience resolved discrepancies and validated question design, ensuring that all questions genuinely assess MLLM capabilities.

Visual Grounding In XLRs-Bench, we evaluated visual grounding across two L-3 dimensions. We analyze each image by selecting 5-10 objects per L-3 dimension, resulting in 10-20 objects per image. Concretely, we carefully crafted reference sentences for each object to enable independent and precise identification. Distinctive features in these sentences such as color, shape, position, size, and relative spatial attributes distinguished each reference object from others. For the *Condition-based Visual Grounding* task, annotators used detailed image information to create specific descriptions of conditions, including possible constraints on state or geographic details. Notably, all visual grounding annotations were performed by the annotation and quality control team of the VQA group, ensuring high-quality manual annotation throughout.

Image Caption Unlike other approaches that assess MLLM’s understanding of RS images with single, simple descriptions, we believe the rich details in ultra-high-resolution images require thorough and precise descriptions. For captioning, we use a semi-automated pipeline to interpret and generate text annotations of the image, as shown in Figure 4. We begin by dividing each image into nine sub-images, as using GPT-based tools to annotate the entire image often results in low-quality captions that lose important details, whereas the sub-image approach helps mitigate this issue.

In the next steps, we input 10 images (nine sub-images plus a compressed full image) into GPT-4o using complex prompts to generate detailed and comprehensive captions. For instance, for a $10,000 \times 10,000$ image where a river spans the scene with a wetland on one side and urban areas on the other, using sub-images alone cannot reflect the river’s flow and overall layout, while only adopting the full image lacks local details. Our combined input method ad-

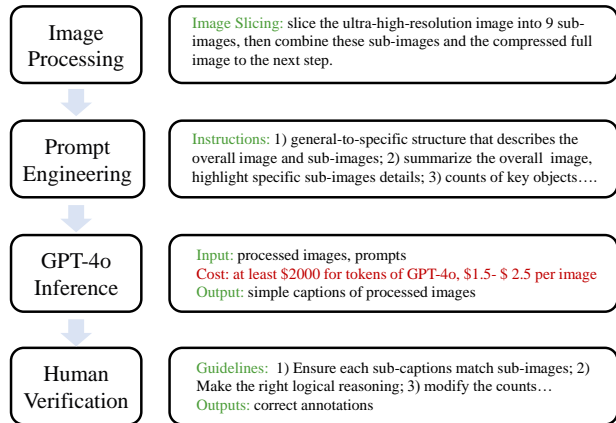


Figure 4. Semi-automated pipeline for detailed image captioning in XLRs-Bench.

resses both problems. For the ultra-high-resolution RS scenarios, we adopt a general-to-specific structure that separately describes the overall image and each sub-image, where the key objects in the description of sub-images (like vehicles, boats, and buildings) are counted. Then we require the GPT-4o to count and display prominent objects across the entire image, identify anomalies, and predict potential risks or developments. Detailed captions and multi-image inputs resulted in extensive token usage with GPT-4o, costing over \$2,000 for captioning 1,000 images. However, despite precise prompts, GPT-4 still struggles with complex tasks such as counting and reasoning, necessitating substantial human intervention to ensure the quality of the captions. To address this, annotators refine the captions using existing VQA annotations for detail and quality control. These refinements include adjusting summaries, correcting object counts, refining scene types, ordering regional descriptions by prominence, and manually annotating anomalies.

3.3. Analysis

Resolution. There are some benchmarks that adopt the image with sizes up to $2,000 \times 1,500$ pixels, but they are primarily designed for natural images rather than RS scenes. In contrast, current RS benchmarks typically remain below 512×512 pixels, as shown in Table 1. In contrast, our XLRs-Bench, with an average size of $8,500 \times 8,500$ pixels, provides extensive views that facilitate a deeper understanding of real RS scenarios. Remarkably, it includes 840 images at $10,000 \times 10,000$ pixels, producing over 10,000 QA pairs. In fact, even annotators must carefully analyze these images to answer questions, with cross-validation employed to reduce errors. We hope this large-size RS benchmark is able to drive the development of MLLMs.

Length of Caption. XLRs-Bench offers comprehensive descriptions that cover global image context, regional details, specific object attributes, object counts, anomalies,

Table 2. Experimental results on the perception and reasoning dimensions of VQA tasks, with models ranked by average performance. Proprietary models are highlighted in gray. ‘Avg’ represents the average accuracy across sub-tasks.

Method	LLM	Language	Perception				Reasoning				Avg.
			Sub-tasks (L-2 Capability)	Counting	Scene Classification	Object Spatial Relationship	Object Properties	Complex Reasoning	Planning	Spatiotemporal Reasoning	
CogVLM2	Llama3-8B	en	36.66	46.26	35.92	36.89	60.23	34.16	-	69.85	39.80
Qwen2-VL	Qwen2-7B	en	39.72	48.30	32.04	35.07	64.23	32.12	45.93	68.35	38.99
LLaVA-OneVision	Qwen2-7B	en	35.84	47.76	32.60	35.95	60.37	24.07	37.78	71.88	38.90
GPT-4o-mini	-	en	28.32	45.46	29.96	36.29	54.84	33.81	15.19	72.06	37.99
InternVL2	InternLM2.5-7B	en	33.91	44.93	26.60	34.84	66.43	33.01	44.44	74.54	37.89
InternLM-XComposer-2.5	InternLM2-7B	en	35.84	47.43	32.75	30.60	64.76	35.31	32.22	69.50	36.33
LLaVA-Next	Llama3-8B	en	38.00	40.79	32.50	31.22	61.85	26.02	32.22	69.10	35.65
GPT-4o	-	en	29.51	48.55	32.35	24.78	52.60	41.24	21.85	72.06	32.15
LLaVA-1.5	Vicuna-7B	en	22.65	19.69	23.05	20.21	33.86	38.67	29.26	34.70	22.81
GeoChat	Vicuna-7B	en	22.65	18.96	23.30	20.21	30.33	32.23	-	33.25	22.03
Qwen2-VL	Qwen2-7B	zh	39.49	49.28	33.26	37.89	67.62	24.34	44.44	76.57	41.10
InternVL2	InternLM2.5-7B	zh	34.42	39.12	34.24	37.54	68.57	40.09	44.07	76.57	40.58
LLaVA-OneVision	Qwen2-7B	zh	37.48	47.06	31.73	34.72	62.56	29.12	30.37	74.80	38.42
GPT-4o-mini	-	zh	29.51	44.13	29.59	35.41	55.36	41.86	21.85	74.71	37.82
InternLM-XComposer-2.5	InternLM2-7B	zh	37.70	43.15	32.62	33.40	62.99	29.47	24.44	69.14	37.26
CogVLM2	Llama3-8B	zh	36.21	45.79	34.57	31.03	59.56	26.19	-	70.47	35.84
LLaVA-Next	Llama3-8B	zh	33.08	39.52	31.98	29.34	54.07	21.59	25.56	69.85	33.48
GPT-4o	-	zh	22.28	45.47	31.25	24.93	45.45	27.08	15.19	69.41	30.40
LLaVA-1.5	Vicuna-7B	zh	22.65	19.07	23.01	20.21	33.95	38.67	29.26	37.58	22.86
GeoChat	Vicuna-7B	zh	22.65	19.17	23.05	20.21	24.75	22.79	-	23.74	20.99

Table 3. Detailed image captioning performance on XLRs-Bench.

Method	Language	BLEU-1	BLEU-2	BLEU-3	BLEU-4	METEOR	ROUGEL
GeoChat	en	16.74	8.38	4.49	2.45	10.37	16.72
GPT-4o	en	34.69	17.67	8.56	4.04	23.54	20.93
GPT-4o-mini	en	38.29	19.75	9.76	4.29	23.94	21.30
Qwen2-VL	en	26.74	12.79	5.99	2.53	19.32	19.76
LLaVA-OneVision	en	41.12	20.42	9.94	4.56	19.99	21.03
LLaVA-Next	en	27.62	13.45	6.82	3.52	17.78	20.65
LLaVA-1.5	en	35.82	17.62	8.92	4.33	16.49	20.80
CogVLM2	en	30.27	14.46	6.80	3.09	19.37	19.17
InternLM-XComposer-2.5	en	35.17	15.91	7.00	3.02	19.99	17.95
InternVL2	en	25.71	12.44	5.84	2.58	19.55	19.43
GeoChat	zh	6.77	1.49	0.68	0.26	7.84	15.79
GPT-4o	zh	31.08	3.86	1.43	0.43	26.41	36.41
GPT-4o-mini	zh	34.13	5.37	2.20	0.58	25.73	37.11
Qwen2-VL	zh	21.80	3.50	1.41	0.33	22.92	31.04
LLaVA-OneVision	zh	33.05	5.67	2.47	0.98	20.24	31.95
LLaVA-Next	zh	13.01	2.10	0.82	0.20	15.12	27.72
LLaVA-1.5	zh	28.56	4.26	1.73	0.00	16.36	29.18
CogVLM2	zh	19.78	2.23	0.79	0.18	22.53	28.33
InternLM-XComposer-2.5	zh	37.30	6.12	2.39	0.58	20.86	32.97
InternVL2	zh	16.49	3.16	1.39	0.48	22.10	25.76

and reasoning information. Each caption starts with a general image overview, followed by precise details across various regions. Regional details include object attributes such as count, color, shape, size, and spatial positioning—both absolute values within the image and relative to other objects like buildings, roads, and trees. In summary, these descriptions emphasize clear, distinct features, avoiding ambiguity, and typically average 19 sentences (379 words) in English and 20 sentences (663 words) in Chinese.

Bilingual. Traditional VQA methods [34] use translation engines to convert QA pairs from English to Chinese, but this often leads to visual-text misalignment [54] and fails to handle subtleties, contextual nuances, language bias, and diverse question types. These issues are particularly evident in detailed captioning, where long content makes machine translation prone to errors. To build a high-quality Chinese benchmark, we engaged six bilingual experts fluent in Chinese and English to translate and cross-check all long-text content. Finally, 1,400 images, 32,389 QA pairs, 12,619 groundings, and 934 detailed captions are served for the Chinese version of XLRs-Bench, maintaining similar task types, image quality, and difficulty.

4. Experiment

4.1. Experimental Setup

The MLLMs evaluated on XLRs-Bench are grouped into three categories: (a) open-source VLMs, including Qwen2-VL [63], LLaVA-Onevision [27], LLaVA-Next [32], LLaVA-1.5 [58], CogVLM2 [18], InternLM-XComposer-2.5 [73] and InternVL-2 [64]; (b) closed-source VLMs, such as GPT-4o [42] and GPT-4o-mini [43]; and (c) the specialized RS model GeoChat [23]. For fair comparison, we used a zero-shot setting with uniform prompts for all VLMs. The appendix details the architecture and parameter sizes of each open-source VLM and includes additional results across various settings. Except for GeoChat which was evaluated using its native framework, all other models were evaluated using LMMs-Eval [26, 71]. More results are shown in the Appendix.

4.2. Evaluation Strategy

In the VQA task, we manually created four options for each question: one correct answer and three distractors, derived from text within the image or similar alternatives. This increases the difficulty by requiring models to deeply understand image details. Following MMBench [34] and MME-Realworld [77] methods, we evaluated the accuracy of L-2 capability dimension for the VQA task and reported the average accuracy across L-2 dimensions, with L-3 results available in the appendix. For the L3 sub-task of Overall Land Use Classification, where a question may have multiple correct options, a prediction is considered correct only if it matches the ground truth exactly. For the Grounding task, we used precision, assessing accuracy based on the intersection between predicted and ground truth bounding boxes, with predictions deemed correct if IoU exceeds a threshold. We tested two IoU thresholds: 0.5 and 0.7. For the caption-

Table 4. Visual grounding performance on XLRs-Bench and VRSBench [28]. *: VRSBench uses GPT-4V to assess this task.

Benchmark	Method	GPT-4o*	GPT-4o-mini	Qwen2-VL	LLaVA-OneVision	LLaVA-Next	LLaVA-1.5	CogVLM2	InternLM-XComposer-2.5	InternVL2	GeoChat
XLRs-Bench-EN	Acc@0.5	0.46	0.09	0.15	0.16	0.18	0.09	0.01	0.02	0.33	0.14
	Acc@0.7	0.05	0.03	0.03	0.00	0.04	0.00	0.00	0.01	0.12	0.01
XLRs-Bench-ZH	Acc@0.5	0.45	0.21	0.14	0.13	0.07	0.12	0.03	0.06	0.19	0.14
	Acc@0.7	0.03	0.03	0.01	0.01	0.02	0.02	0.00	0.00	0.06	0.01
VRSBench	Acc@0.5	5.1	-	-	-	-	-	-	-	-	-
	Acc@0.7	1.1	-	-	-	-	-	-	-	-	-

ing task, we used standard metrics, including BLEU [46], ROUGE_L [9], and METEOR [4]. We consider the n-gram precision for BLEU with n-values of 1, 2, 3, and 4. All scores in Tables 2, 3, and 4 are reported as percentages (%).

4.3. Main Results

Results on VQA tasks. Table 2 compares various models on the different four L-2 dimensions of perception and reasoning abilities, respectively. Qwen2-VL excels in both English and Chinese proficiency, outperforming both proprietary and most open-source models. Nevertheless, their performance varies across tasks. From the results, we can draw the following key insights: (1) *GPT-4o’s Weakness in Spatiotemporal Reasoning*: GPT-4o underperforms compared to open-source models on complex spatiotemporal reasoning tasks, with accuracy consistently below 25%. These tasks, focused on local counting for change detection, assess MLLMs’ ability to capture temporal details across images. GPT-4o likely lacks pretraining on RS scene change detection and sometimes refuses to answer questions citing privacy or harmful content. By contrast, Qwen2-VL performs reliably on these sub-tasks. (2) *Benefits of Higher-Resolution Input Models*: Models like Qwen2-VL, which allow higher-resolution inputs, significantly outperform those using visual encoders like CLIP (e.g., LLaVA1.5). The limit of input image size often necessitates compression, but Qwen2-VL’s ability to process richer information at larger image sizes leads to superior performance. (3) *Better Abstract Reasoning in RS*: In high-resolution RS scenarios, models excel at abstract reasoning tasks like anomaly detection, which require minimal local detail and can rely on compressed regional data. Conversely, for perception-heavy tasks requiring fine detail recognition, MLLMs are constrained by their architecture, achieving accuracy rates of only 30%–50%.

Results on image captioning tasks. Our captions have average 1379 words in English and 663 in Chinese, offering richly detailed descriptions with broad applicability. However, evaluations show MLLMs struggle with these lengthy, real-world captions; open-source models like Qwen2-VL and the RS-specific GeoChat perform poorly. Notably, GPT-4o and GPT-4o-mini, even without extensive RS pretraining, excel in long-text generation, significantly outperforming other models. Previous evaluations in RS captioning focused on shorter texts, missing GPT-4o’s strengths with longer content. For Chinese caption tasks, GPT-4o still outperforms other models, showcasing its robust understanding and generation abilities as a valuable as-

set for future research.

Results on grounding tasks. While we anticipated challenges in visual localization during annotation, the poor performance of each MLLM was surprising. To validate the benchmark’s effectiveness, we conducted additional human verification: we randomly selected 100 questions from each VQA sub-task (L-3 dimensions) and had two groups answer them concurrently. We also included results from the low-resolution RS visual grounding dataset, VRSBench. Notably, even in 512×512 low-resolution RS scenarios, GPT-4V achieved only 1.1% and 5.1% accuracy; when scaled to resolutions near $8,500 \times 8,500$, the accuracy rates of 3.2% and 0.48% are understandable. Some objects in these large images are as small as 5–10 pixels, posing a challenge for current MLLMs.

Limitations and discussions. 1) *Limitations in Spatiotemporal Understanding*: General models (like LLaVA-series and GPT-4o) lack large-scale training tailored to RS spatiotemporal understandings, leading to poor performance on such tasks. For instance, GPT-4o achieves less than 25% accuracy (Table 2). Given the widespread application of these tasks in RS, domain-specific training is essential. Specialized models like GeoChat have yet to support multi-image input tasks, highlighting the need for further research in this area. 2) *Challenges in Ultra-High-Resolution Scenarios*: Current high-resolution MLLMs are limited to 4K images, requiring significant compression for larger-size images, resulting in substantial information loss. This issue is critical for satellite imagery, where the small objects are often measured only 5–10 pixels and shrink to a single pixel after compression, rendering them uninformative. Developing specialized MLLMs for RS super-resolution is anticipated to mitigate this limitation.

5. Conclusion

In this paper, we introduce XLRs-Bench, a comprehensive benchmark for evaluating the perception and reasoning capabilities of multimodal large language models (MLLMs) in ultra-high-resolution remote sensing (RS) scenarios. XLRs-Bench features the largest average image size to date, high-quality human-verified annotations, and 16 sub-tasks across three ability levels, offering a multidimensional evaluation. It supports both English and Chinese, making it the largest manually annotated ultra-high-resolution RS vision-language dataset, surpassing existing benchmarks in data capacity and task diversity. By emphasizing real-world decision-making and spatiotemporal

change detection, XLRs-Bench promotes advanced cognitive processes. Experimental results demonstrate that current general-purpose and RS-specific MLLMs still struggle to understand ultra-high-resolution RS imagery, underscoring the need for further improvements.

6. Acknowledgements

This work was partially supported by the National Natural Science Foundation of China (No. 62372459, No.62376282 and No. 624B2109)

References

- [1] Harsh Agrawal, Karan Desai, Yufei Wang, Xinlei Chen, Rishabh Jain, Mark Johnson, Dhruv Batra, Devi Parikh, Stefan Lee, and Peter Anderson. Nocaps: Novel object captioning at scale. In *Proceedings of the IEEE/CVF international conference on computer vision*, pages 8948–8957, 2019. 3
- [2] Jinze Bai, Shuai Bai, Shusheng Yang, Shijie Wang, Sinan Tan, Peng Wang, Junyang Lin, Chang Zhou, and Jingren Zhou. Qwen-vl: A frontier large vision-language model with versatile abilities. *arXiv preprint arXiv:2308.12966*, 2023. 2, 3
- [3] Shuai Bai, Shusheng Yang, Jinze Bai, Peng Wang, Xingxuan Zhang, Junyang Lin, Xinggang Wang, Chang Zhou, and Jingren Zhou. Touchstone: Evaluating vision-language models by language models. *arXiv preprint arXiv:2308.16890*, 2023. 5
- [4] Satanjeev Banerjee and Alon Lavie. Meteor: An automatic metric for mt evaluation with improved correlation with human judgments. In *Proceedings of the acl workshop on intrinsic and extrinsic evaluation measures for machine translation and/or summarization*, pages 65–72, 2005. 8
- [5] Yonatan Bitton, Hritik Bansal, Jack Hessel, Rulin Shao, Wanrong Zhu, Anas Awadalla, Josh Gardner, Rohan Taori, and Ludwig Schimdt. Visit-bench: a benchmark for vision-language instruction following inspired by real-world use. In *Proceedings of the 37th International Conference on Neural Information Processing Systems*, pages 26898–26922, 2023. 2, 5
- [6] Javier Castillo-Navarro, Bertrand Le Saux, Alexandre Boulch, Nicolas Audebert, and Sébastien Lefèvre. Semi-supervised semantic segmentation in earth observation: The minifrance suite, dataset analysis and multi-task network study. *Machine Learning*, 111(9):3125–3160, 2022. 2, 5, 35, 36
- [7] Lin Chen, Jinsong Li, Xiaoyi Dong, Pan Zhang, Yuhang Zang, Zehui Chen, Haodong Duan, Jiaqi Wang, Yu Qiao, Dahua Lin, et al. Are we on the right way for evaluating large vision-language models? *arXiv preprint arXiv:2403.20330*, 2024. 5
- [8] Xinlei Chen, Hao Fang, Tsung-Yi Lin, Ramakrishna Vedantam, Saurabh Gupta, Piotr Dollár, and C Lawrence Zitnick. Microsoft coco captions: Data collection and evaluation server. *arXiv preprint arXiv:1504.00325*, 2015. 3
- [9] Lin Chin-Yew. Rouge: A package for automatic evaluation of summaries. In *Proceedings of the Workshop on Text Summarization Branches Out, 2004*, 2004. 8
- [10] Rodrigo Caye Daudt, Bertrand Le Saux, Alexandre Boulch, and Yann Gousseau. Multitask learning for large-scale semantic change detection. *Computer Vision and Image Understanding*, 187:102783, 2019. 3, 5, 35, 36
- [11] Fabio Dell’Acqua and Paolo Gamba. Remote sensing and earthquake damage assessment: Experiences, limits, and perspectives. *Proceedings of the IEEE*, 100(10):2876–2890, 2012. 2
- [12] Chaoyou Fu, Peixian Chen, Yunhang Shen, Yulei Qin, Mengdan Zhang, Xu Lin, Jinrui Yang, Xiawu Zheng, Ke Li, Xing Sun, et al. Mme: A comprehensive evaluation benchmark for multimodal large language models. *arXiv preprint arXiv:2306.13394*, 2023. 2, 3, 5
- [13] Xingyu Fu, Yushi Hu, Bangzheng Li, Yu Feng, Haoyu Wang, Xudong Lin, Dan Roth, Noah A Smith, Wei-Chiu Ma, and Ranjay Krishna. Blink: Multimodal large language models can see but not perceive. In *European Conference on Computer Vision*, pages 148–166. Springer, 2024. 2, 5
- [14] Timnit Gebru, Jamie Morgenstern, Briana Vecchione, Jennifer Wortman Vaughan, Hanna Wallach, Hal Daumé Iii, and Kate Crawford. Datasheets for datasets. *Communications of the ACM*, 64(12):86–92, 2021. 35
- [15] Yash Goyal, Tejas Khot, Douglas Summers-Stay, Dhruv Batra, and Devi Parikh. Making the v in vqa matter: Elevating the role of image understanding in visual question answering. In *Proceedings of the IEEE conference on computer vision and pattern recognition*, pages 6904–6913, 2017. 3
- [16] Zonghao Guo, Ruyi Xu, Yuan Yao, Junbo Cui, Zanlin Ni, Chunjiang Ge, Tat-Seng Chua, Zhiyuan Liu, and Gao Huang. Llava-uhd: an lmm perceiving any aspect ratio and high-resolution images. In *European Conference on Computer Vision*, pages 390–406. Springer, 2024. 2, 3
- [17] Danna Gurari, Qing Li, Abigale J Stangl, Anhong Guo, Chi Lin, Kristen Grauman, Jiebo Luo, and Jeffrey P Bigham. Vizwiz grand challenge: Answering visual questions from blind people. In *Proceedings of the IEEE conference on computer vision and pattern recognition*, pages 3608–3617, 2018. 3
- [18] Wenyi Hong, Weihang Wang, Ming Ding, Wenmeng Yu, Qingsong Lv, Yan Wang, Yean Cheng, Shiyu Huang, Junhui Ji, Zhao Xue, et al. Cogvlm2: Visual language models for image and video understanding. *arXiv preprint arXiv:2408.16500*, 2024. 7
- [19] Shengding Hu, Yuge Tu, Xu Han, Chaoqun He, Ganqu Cui, Xiang Long, Zhi Zheng, Yewei Fang, Yuxiang Huang, Weilin Zhao, et al. Minicpm: Unveiling the potential of small language models with scalable training strategies. *arXiv preprint arXiv:2404.06395*, 2024. 3
- [20] Yuan Hu, Jianlong Yuan, Congcong Wen, Xiaonan Lu, and Xiang Li. Rsgpt: A remote sensing vision language model and benchmark. *arXiv preprint arXiv:2307.15266*, 2023. 3, 5
- [21] Liang Huang, Fengxiang Wang, Yalun Zhang, and Qingxia Xu. Fine-grained ship classification by combining cnn and swin transformer. *Remote Sensing*, 14(13):3087, 2022. 3

- [22] Drew A Hudson and Christopher D Manning. Gqa: A new dataset for real-world visual reasoning and compositional question answering. In *Proceedings of the IEEE/CVF conference on computer vision and pattern recognition*, pages 6700–6709, 2019. 3
- [23] Kartik Kuckreja, Muhammad Sohail Danish, Muzammal Naseer, Abhijit Das, Salman Khan, and Fahad Shahbaz Khan. Geochat: Grounded large vision-language model for remote sensing. In *Proceedings of the IEEE/CVF Conference on Computer Vision and Pattern Recognition*, pages 27831–27840, 2024. 3, 7, 18
- [24] Long Lan, Fengxiang Wang, Xiangtao Zheng, Zengmao Wang, and Xinwang Liu. Efficient prompt tuning of large vision-language model for fine-grained ship classification. *IEEE Transactions on Geoscience and Remote Sensing*, 2024. 3
- [25] Bohao Li, Rui Wang, Guangzhi Wang, Yuying Ge, Yixiao Ge, and Ying Shan. Seed-bench: Benchmarking multimodal llms with generative comprehension. *arXiv preprint arXiv:2307.16125*, 2023. 2, 3, 5, 13
- [26] Bo Li, Peiyuan Zhang, Kaichen Zhang, Fanyi Pu, Xinrun Du, Yuhao Dong, Haotian Liu, Yuanhan Zhang, Ge Zhang, Chunyuan Li, and Ziwei Liu. Lmms-eval: Accelerating the development of large multimodal models. <https://github.com/EvolvingLMs-Lab/lmms-eval>, 2024. 7, 35
- [27] Bo Li, Yuanhan Zhang, Dong Guo, Renrui Zhang, Feng Li, Hao Zhang, Kaichen Zhang, Yanwei Li, Ziwei Liu, and Chunyuan Li. Llava-onevision: Easy visual task transfer. *arXiv preprint arXiv:2408.03326*, 2024. 7
- [28] Xiang Li, Jian Ding, and Mohamed Elhoseiny. Vrsbench: A versatile vision-language benchmark dataset for remote sensing image understanding. *arXiv preprint arXiv:2406.12384*, 2024. 2, 3, 4, 5, 8, 37
- [29] Yanwei Li, Yuechen Zhang, Chengyao Wang, Zhisheng Zhong, Yixin Chen, Ruihang Chu, Shaoteng Liu, and Jiaya Jia. Mini-gemini: Mining the potential of multi-modality vision language models. *arXiv preprint arXiv:2403.18814*, 2024. 2, 3
- [30] Zhang Li, Biao Yang, Qiang Liu, Zhiyin Ma, Shuo Zhang, Jingxu Yang, Yabo Sun, Yuliang Liu, and Xiang Bai. Monkey: Image resolution and text label are important things for large multi-modal models. In *proceedings of the IEEE/CVF conference on computer vision and pattern recognition*, pages 26763–26773, 2024. 3
- [31] Haotian Liu, Chunyuan Li, Qingyang Wu, and Yong Jae Lee. Visual instruction tuning. *Advances in neural information processing systems*, 36:34892–34916, 2023. 3
- [32] Haotian Liu, Chunyuan Li, Yuheng Li, Bo Li, Yuanhan Zhang, Sheng Shen, and Yong Jae Lee. Llava-next: Improved reasoning, ocr, and world knowledge. <https://llava-vl.github.io/blog/2024-01-30-llava-next1>, 2024. 2, 3, 7
- [33] Sihan Liu, Yiwei Ma, Xiaoqing Zhang, Haowei Wang, Jiayi Ji, Xiaoshuai Sun, and Rongrong Ji. Rotated multi-scale interaction network for referring remote sensing image segmentation. In *Proceedings of the IEEE/CVF Conference on Computer Vision and Pattern Recognition*, 2024. 5
- [34] Yuan Liu, Haodong Duan, Yuanhan Zhang, Bo Li, Songyang Zhang, Wangbo Zhao, Yike Yuan, Jiaqi Wang, Conghui He, Ziwei Liu, et al. Mmbench: Is your multi-modal model an all-around player? In *European conference on computer vision*, pages 216–233. Springer, 2024. 2, 3, 5, 7, 13, 15
- [35] Sylvain Lobry, Diego Marcos, Jesse Murray, and Devis Tuia. Rsvqa: Visual question answering for remote sensing data. *IEEE Transactions on Geoscience and Remote Sensing*, 58(12):8555–8566, 2020. 5
- [36] Xiaoqiang Lu, Binqiang Wang, Xiangtao Zheng, and Xuelong Li. Exploring models and data for remote sensing image caption generation. *IEEE Transactions on Geoscience and Remote Sensing*, 56(4):2183–2195, 2017. 5
- [37] Junwei Luo, Zhen Pang, Yongjun Zhang, Tingzhu Wang, Linlin Wang, Bo Dang, Jiangwei Lao, Jian Wang, Jingdong Chen, Yihua Tan, et al. Skysensegpt: A fine-grained instruction tuning dataset and model for remote sensing vision-language understanding. *arXiv preprint arXiv:2406.10100*, 2024. 3
- [38] Kenneth Marino, Mohammad Rastegari, Ali Farhadi, and Roozbeh Mottaghi. Ok-vqa: A visual question answering benchmark requiring external knowledge. In *Proceedings of the IEEE/cvf conference on computer vision and pattern recognition*, pages 3195–3204, 2019. 3
- [39] Valerio Marsocci, Yuru Jia, Georges Le Bellier, David Kerekes, Liang Zeng, Sebastian Hafner, Sebastian Gerard, Eric Brune, Ritu Yadav, Ali Shibli, et al. Pangaea: A global and inclusive benchmark for geospatial foundation models. *arXiv preprint arXiv:2412.04204*, 2024. 3
- [40] Ahmed Masry, Do Xuan Long, Jia Qing Tan, Shafiq Joty, and Enamul Hoque. Chartqa: A benchmark for question answering about charts with visual and logical reasoning. *arXiv preprint arXiv:2203.10244*, 2022. 13
- [41] Dilxat Muhtar, Zhenshi Li, Feng Gu, Xueliang Zhang, and Pengfeng Xiao. Lhrs-bot: Empowering remote sensing with vgi-enhanced large multimodal language model. In *European Conference on Computer Vision*, pages 440–457. Springer, 2024. 2, 3
- [42] OpenAI. Hello gpt-4o. <https://openai.com/index/hello-gpt-4o>, 2024. 7
- [43] OpenAI. Gpt-4o mini: advancing cost-efficient intelligence. <https://openai.com/index/gpt-4o-mini-advancing-cost-efficient-intelligence>, 2024. 7
- [44] OpenAI, Josh Achiam, Steven Adler, Sandhini Agarwal, Lama Ahmad, Ilge Akkaya, Florencia Leoni Aleman, Diogo Almeida, Janko Altenschmidt, Sam Altman, et al. Gpt-4 technical report. *arXiv preprint arXiv:2303.08774*, 2024. 2, 3
- [45] Chao Pang, Jiang Wu, Jiayu Li, Yi Liu, Jiaying Sun, Weijia Li, Xingxing Weng, Shuai Wang, Litong Feng, Gui-Song Xia, et al. H2rsvlm: Towards helpful and honest remote sensing large vision language model. *arXiv preprint arXiv:2403.20213*, 2024. 3
- [46] Kishore Papineni, Salim Roukos, Todd Ward, and Wei-Jing Zhu. Bleu: a method for automatic evaluation of machine translation. In *Proceedings of the 40th annual meeting of the*

- Association for Computational Linguistics*, pages 311–318, 2002. 8
- [47] Bo Qu, Xuelong Li, Dacheng Tao, and Xiaoqiang Lu. Deep semantic understanding of high resolution remote sensing image. In *2016 International conference on computer, information and telecommunication systems (Cits)*, pages 1–5. IEEE, 2016. 5
- [48] Franz Rottensteiner, Gunho Sohn, Markus Gerke, and Jan D Wegner. Isprs semantic labeling contest. *ISPRS: Leopoldshöhe, Germany*, 1(4):4, 2014. 5
- [49] Franz Rottensteiner, Gunho Sohn, Markus Gerke, Jan Dirk Wegner, Uwe Breitkopf, and Jaewook Jung. Results of the isprs benchmark on urban object detection and 3d building reconstruction. *ISPRS journal of photogrammetry and remote sensing*, 93:256–271, 2014. 5
- [50] Tanik Saikh, Tirthankar Ghosal, Amish Mittal, Asif Ekbal, and Pushpak Bhattacharyya. Scienceqa: A novel resource for question answering on scholarly articles. *International Journal on Digital Libraries*, 23(3):289–301, 2022. 5
- [51] Amanpreet Singh, Vivek Natarajan, Meet Shah, Yu Jiang, Xinlei Chen, Dhruv Batra, Devi Parikh, and Marcus Rohrbach. Towards vqa models that can read. In *CVPR*, 2019. 13
- [52] Amanpreet Singh, Vivek Natarajan, Meet Shah, Yu Jiang, Xinlei Chen, Dhruv Batra, Devi Parikh, and Marcus Rohrbach. Towards vqa models that can read. In *Proceedings of the IEEE/CVF conference on computer vision and pattern recognition*, pages 8317–8326, 2019. 3
- [53] Yuxi Sun, Shanshan Feng, Xutao Li, Yunming Ye, Jian Kang, and Xu Huang. Visual grounding in remote sensing images. In *Proceedings of the 30th ACM International Conference on Multimedia*, pages 404–412, 2022. 5
- [54] Jingqun Tang, Qi Liu, Yongjie Ye, Jinghui Lu, Shu Wei, Chunhui Lin, Wanqing Li, Mohamad Fitri Faiz Bin Mahmood, Hao Feng, Zhen Zhao, et al. Mtvqa: Benchmarking multilingual text-centric visual question answering. *arXiv preprint arXiv:2405.11985*, 2024. 7
- [55] Gemini Team, Rohan Anil, Sebastian Borgeaud, Yonghui Wu, Jean-Baptiste Alayrac, Jiahui Yu, Radu Soricut, Johan Schalkwyk, Andrew M Dai, Anja Hauth, et al. Gemini: a family of highly capable multimodal models. *arXiv preprint arXiv:2312.11805*, 2023. 2, 3
- [56] Peter Tong, Ellis Brown, Penghao Wu, Sanghyun Woo, Adithya Jairam Vedagiri IYER, Sai Charitha Akula, Shusheng Yang, Jihan Yang, Manoj Middepogu, Ziteng Wang, et al. Cambrian-1: A fully open, vision-centric exploration of multimodal llms. *Advances in Neural Information Processing Systems*, 37:87310–87356, 2024. 2, 5
- [57] Shengbang Tong, Ellis Brown, Penghao Wu, Sanghyun Woo, Manoj Middepogu, Sai Charitha Akula, Jihan Yang, Shusheng Yang, Adithya Iyer, Xichen Pan, et al. Cambrian-1: A fully open, vision-centric exploration of multimodal llms. *arXiv preprint arXiv:2406.16860*, 2024. 3
- [58] Hugo Touvron, Thibaut Lavril, Gautier Izacard, Xavier Martinet, Marie-Anne Lachaux, Timothée Lacroix, Baptiste Rozière, Naman Goyal, Eric Hambro, Faisal Azhar, et al. Llama: Open and efficient foundation language models. *arXiv preprint arXiv:2302.13971*, 2023. 2, 3, 7
- [59] Boxin Wang, Weixin Chen, Hengzhi Pei, Chulin Xie, Mintong Kang, Chenhui Zhang, Chejian Xu, Zidi Xiong, Ritik Dutta, Rylan Schaeffer, et al. Decodingtrust: A comprehensive assessment of trustworthiness in gpt models. In *NeurIPS*, 2023. 3
- [60] Fengxiang Wang, Wanrong Huang, Shaowu Yang, Qi Fan, and Long Lan. Learning to learn better visual prompts. *Proceedings of the AAAI Conference on Artificial Intelligence*, 38(6):5354–5363, 2024. 3
- [61] Fengxiang Wang, Hongzhen Wang, Di Wang, Zonghao Guo, Zhenyu Zhong, Long Lan, Jing Zhang, Zhiyuan Liu, and Maosong Sun. Scaling efficient masked autoencoder learning on large remote sensing dataset. *arXiv preprint arXiv:2406.11933*, 2024. 3
- [62] Fengxiang Wang, Hongzhen Wang, Yulin Wang, Di Wang, Mingshuo Chen, Haiyan Zhao, Yangang Sun, Shuo Wang, Long Lan, Wenjing Yang, et al. Roma: Scaling up mamba-based foundation models for remote sensing. *arXiv preprint arXiv:2503.10392*, 2025. 3
- [63] Peng Wang, Shuai Bai, Sinan Tan, Shijie Wang, Zhihao Fan, Jinze Bai, Keqin Chen, Xuejing Liu, Jialin Wang, Wenbin Ge, et al. Qwen2-vl: Enhancing vision-language model’s perception of the world at any resolution. *arXiv preprint arXiv:2409.12191*, 2024. 7
- [64] Weiyun Wang, Zhe Chen, Wenhai Wang, Yue Cao, Yangzhou Liu, Zhangwei Gao, Jinguo Zhu, Xizhou Zhu, Lewei Lu, Yu Qiao, et al. Enhancing the reasoning ability of multimodal large language models via mixed preference optimization. *arXiv preprint arXiv:2411.10442*, 2024. 7
- [65] Gui-Song Xia, Xiang Bai, Jian Ding, Zhen Zhu, Serge Be-longie, Jiebo Luo, Mihai Datcu, Marcello Pelillo, and Liang-pei Zhang. Dota: A large-scale dataset for object detection in aerial images. In *Proceedings of the IEEE conference on computer vision and pattern recognition*, pages 3974–3983, 2018. 2, 3, 5, 35, 36
- [66] Michael Ying Yang, Wentong Liao, Xinbo Li, and Bodo Rosenhahn. Deep learning for vehicle detection in aerial images. In *2018 25th IEEE International Conference on Image Processing (ICIP)*, pages 3079–3083. IEEE, 2018. 5, 35, 36
- [67] Kaining Ying, Fanqing Meng, Jin Wang, Zhiqian Li, Han Lin, Yue Yang, Hao Zhang, Wenbo Zhang, Yuqi Lin, Shuo Liu, et al. Mmt-bench: A comprehensive multimodal benchmark for evaluating large vision-language models towards multitask agi. In *International Conference on Machine Learning*, pages 57116–57198. PMLR, 2024. 2, 3, 5, 15
- [68] Peter Young, Alice Lai, Micah Hodosh, and Julia Hockenmaier. From image descriptions to visual denotations: New similarity metrics for semantic inference over event descriptions. *Transactions of the Association for Computational Linguistics*, 2:67–78, 2014. 3
- [69] Weihao Yu, Zhengyuan Yang, Linjie Li, Jianfeng Wang, Kevin Lin, Zicheng Liu, Xinchao Wang, and Lijuan Wang. Mm-vet: Evaluating large multimodal models for integrated capabilities. In *International Conference on Machine Learning*, pages 57730–57754. PMLR, 2024. 5
- [70] Yang Zhan, Zhitong Xiong, and Yuan Yuan. Rsvg: Exploring data and models for visual grounding on remote sensing data.

IEEE Transactions on Geoscience and Remote Sensing, 61: 1–13, 2023. [5](#)

- [71] Kaichen Zhang, Bo Li, Peiyuan Zhang, Fanyi Pu, Joshua Adrian Cahyono, Kairui Hu, Shuai Liu, Yuanhan Zhang, Jingkang Yang, Chunyuan Li, and Ziwei Liu. Lmms-eval: Reality check on the evaluation of large multimodal models. *arXiv preprint arXiv:2407.12772*, 2024. [7](#), [35](#)
- [72] Pan Zhang, Xiaoyi Dong Bin Wang, Yuhang Cao, Chao Xu, Linke Ouyang, Zhiyuan Zhao, Shuangrui Ding, Songyang Zhang, Haodong Duan, Hang Yan, et al. Internlm-xcomposer: A vision-language large model for advanced text-image comprehension and composition. *arXiv preprint arXiv:2309.15112*, 2023. [2](#), [3](#)
- [73] Pan Zhang, Xiaoyi Dong, Yuhang Zang, Yuhang Cao, Rui Qian, Lin Chen, Qipeng Guo, Haodong Duan, Bin Wang, Linke Ouyang, et al. Internlm-xcomposer-2.5: A versatile large vision language model supporting long-contextual input and output. *arXiv preprint arXiv:2407.03320*, 2024. [7](#)
- [74] Wei Zhang, Miaoxin Cai, Tong Zhang, Yin Zhuang, and Xuerui Mao. Earthgpt: A universal multi-modal large language model for multi-sensor image comprehension in remote sensing domain. *IEEE Transactions on Geoscience and Remote Sensing*, 2024. [2](#), [3](#)
- [75] X. Zhang, Y. Sun, K. Shang, L. Zhang, and S. Wang. Crop classification based on feature band set construction and object-oriented approach using hyperspectral images. *IEEE J. Sel. Topics Appl. Earth Observ. Remote Sens.*, 9(9):4117–4128, 2016. [2](#)
- [76] Yi-Fan Zhang, Qingsong Wen, Chaoyou Fu, Xue Wang, Zhang Zhang, Liang Wang, and Rong Jin. Beyond llava-hd: Diving into high-resolution large multimodal models. *arXiv preprint arXiv:2406.08487*, 2024. [2](#), [3](#)
- [77] Yi-Fan Zhang, Huanyu Zhang, Haochen Tian, Chaoyou Fu, Shuangqing Zhang, Junfei Wu, Feng Li, Kun Wang, Qingsong Wen, Zhang Zhang, et al. Mme-realworld: Could your multimodal llm challenge high-resolution real-world scenarios that are difficult for humans? *arXiv preprint arXiv:2408.13257*, 2024. [2](#), [3](#), [5](#), [6](#), [7](#), [15](#)
- [78] Xiangtao Zheng, Binqiang Wang, Xingqian Du, and Xiaoqiang Lu. Mutual attention inception network for remote sensing visual question answering. *IEEE Transactions on Geoscience and Remote Sensing*, 60:1–14, 2021. [5](#)
- [79] Luowei Zhou, Chenliang Xu, and Jason Corso. Towards automatic learning of procedures from web instructional videos. In *Proceedings of the AAAI Conference on Artificial Intelligence*, 2018. [3](#)
- [80] Deyao Zhu, Jun Chen, Xiaoqian Shen, Xiang Li, and Mohamed Elhoseiny. Minigt-4: Enhancing vision-language understanding with advanced large language models. In *12th International Conference on Learning Representations, ICLR 2024*, 2024. [2](#), [3](#)
- [81] Zhe Zhu, Yuyu Zhou, Karen C. Seto, Eleanor C. Stokes, Chengbin Deng, Steward T.A. Pickett, and Hannes Taubenböck. Understanding an urbanizing planet: Strategic directions for remote sensing. *Remote Sensing of Environment*, 228:164–182, 2019. [2](#)

A. Appendix

A.1. Overview of the Appendix

This appendix supplements the proposed **XLRS-Bench** with details excluded from the main paper due to space constraints.

The appendix is organized as follows:

- Sec. A.2: More details of XLRS-Bench.
- Sec. A.3: Human evaluations on XLRS-Bench.
- Sec. A.4: More analysis on L-2 capability across various MLLMs.
- Sec. A.5: Detailed results of specific sub-tasks (L-3 capability).
- Sec. A.6: Visualizations of samples and challenging cases.
- Sec. A.7: Datasheets for the XLRS-Bench dataset.
- Sec. A.8: Discussion on limitations and societal impact.

A.2. More Details of XLRS-Bench

We provide additional details about the dataset, with Table 5 presenting statistics for VQA, visual grounding, and image captioning tasks, along with their relationships to the L3 sub-tasks. This clarifies the dataset’s structure and composition. Notably, Visual Grounding spans both perception and reasoning, with Fine-grained Visual Grounding classified under perception and Condition-based Visual Grounding under reasoning.

A.3. Human Evaluations on XLRS-Bench

Human evaluation is essential for assessing dataset effectiveness [34]. For XLRS-Bench, we randomly selected 30 questions from each VQA sub-task (L-3 dimensions) and had two groups answer them simultaneously. The final accuracy was computed as the average accuracy of both groups. Figure 5 illustrates the evaluation results of MLLMs and humans.

We observed that human accuracy consistently exceeded 90%, validating the reliability of XLRS-Bench. However, human evaluation is not error-free, as analyzing large ultra-high-resolution RS images demands intense focus and frequent zooming, particularly for tasks like global counting, making it inherently challenging. In contrast, existing MLLMs, such as the closed-source GPT-4o, performed significantly worse, likely due to insufficient training on real ultra-high-resolution RS data. We encourage future research to address these challenges.

A.4. More Analysis of Results on XLRS-Bench

Due to space limitations, more in-depth analyses to advance MLLM research in ultra-high-resolution remote sensing scenarios are provided in the appendix. This section highlights the performance of all L-2 capabilities.

Most MLLMs underperform across all 16 evaluation dimensions. The accuracy of most MLLMs remains below 50%, in sharp contrast to the 80%–90% typically observed in common benchmarks [25, 34, 40, 51]. Notably, the high accuracy and minimal variation among advanced models in these benchmarks often obscure their practical utility, reducing the significance of small improvements. The consistently low performance on XLRS-Bench underscores the distinct challenges of ultra-high-resolution remote sensing, driven by a lack of pretraining on annotated data. This highlights the pressing need for specialized models to address these complexities.

Performance Gap: Anomaly vs. Spatiotemporal Reasoning A notable performance gap exists between Anomaly Reasoning (AR) and Spatiotemporal Reasoning (SR) tasks. While most models achieve about 70% accuracy on AR tasks, their performance drops sharply to 15.2% on SR tasks. This discrepancy arises because AR tasks depend on identifying global anomalies with clear patterns, whereas SR tasks demand intricate local spatiotemporal modeling. Current MLLMs excel at detecting static anomalies but struggle with dynamic pattern comprehension. To bridge this gap, optimizing MLLMs should focus on improving temporal feature modeling, such as enhancing Transformer architectures to better handle sequential data.

Limited Benefits of Larger LLMs in Perception Tasks. In the Counting and Scene Classification (SC) subtasks, LLaVA-Next (Llama3-8B) offers little advantage over the smaller Qwen2-VL (Qwen2-7B), indicating that model size is not a primary determinant of performance. Instead, factors like diverse pretraining data and effective task alignment mechanisms likely play a more significant role. This underscores the reliance of perception tasks on the visual module’s capabilities rather than the language model’s reasoning. Future efforts could prioritize smaller, more efficient models tailored for perception and explore distillation techniques to enhance visual module performance with reduced model sizes.

Poor Performance in Visual Grounding Tasks. On XLRS-Bench, MLLMs underperform significantly, as shown in main text. On both the Chinese (XLRS-Bench-ZH) and English (XLRS-Bench-EN) benchmarks, most models achieve less than 1.0% accuracy in terms of Acc@0.5 and Acc@0.7 metrics, highlighting major limitations in their ability to handle visual localization tasks. Key issues include: 1. Inadequate local feature extraction, hindering fine-grained localization in ultra-high-resolution images. 2. Weak cross-modal alignment, limiting accurate matching between language descriptions and complex visual scenes. 3. Poor generalization to real-world remote sensing scenarios, particularly with high object similarity. 4. Limited reasoning capability (e.g., condition-based visual grounding, L-3 capability) in ultra-high-resolution set-

Table 5. Characteristics and vision-language formats of L3 sub-tasks.

L1-Task	L2-Task	L3-Task	Abbr.	Annotation Format	Annotation Method	Number of Samples	Answer Type
Perception	Counting	Overall Counting	OC	VQA	All Human	370	Multiple Choice(A/B/C/D)
		Regional Counting	RC	VQA	All Human	972	Multiple Choice(A/B/C/D)
	Scene Classification	Overall Land Use Classification	OLUC	VQA	All Human	904	Multiple Choice(A/B/C/D)
		Regional Land Use Classification	RLUC	VQA	All Human	1854	Multiple Choice(A/B/C/D)
	Object Spatial Relationship	Object Spatial Relationship	OSR	VQA	All Human	4819	Multiple Choice(A/B/C/D)
	Object Properties	Object Classification	OCC	VQA	All Human	9172	Multiple Choice(A/B/C/D)
		Object Color	OCL	VQA	All Human	8930	Multiple Choice(A/B/C/D)
Object Motion State		OMS	VQA	All Human	640	Multiple Choice(A/B for Yes/No)	
Image Captioning	Detailed Image Captioning	-	Caption	Semi-automated	934	Plain Text	
Reasoning	Visual Grounding	Fine-grained Visual Grounding	-	Visual Grounding	All Human	6310	Bounding Box
		Condition-based Visual Grounding	-	Visual Grounding	All Human	6305	Bounding Box
	Route Planning	Route Planning	RP	VQA	All Human	1130	Multiple Choice(A/B/C/D)
	Anomaly Reasoning	Anomaly Detection and Interpretation	AD	VQA	All Human	1131	Multiple Choice(A/B/C/D)
	Complex Reasoning	Environmental Condition Reasoning	ECR	VQA	All Human	1125	Multiple Choice(A/B/C/D)
		Counting with Complex Reasoning	CCR	VQA	All Human	972	Multiple Choice(A/B/C/D)
	Spatiotemporal Reasoning	Regional Counting with Change Detection	RCCD	VQA	All Human	270	Multiple Choice(A/B/C/D)

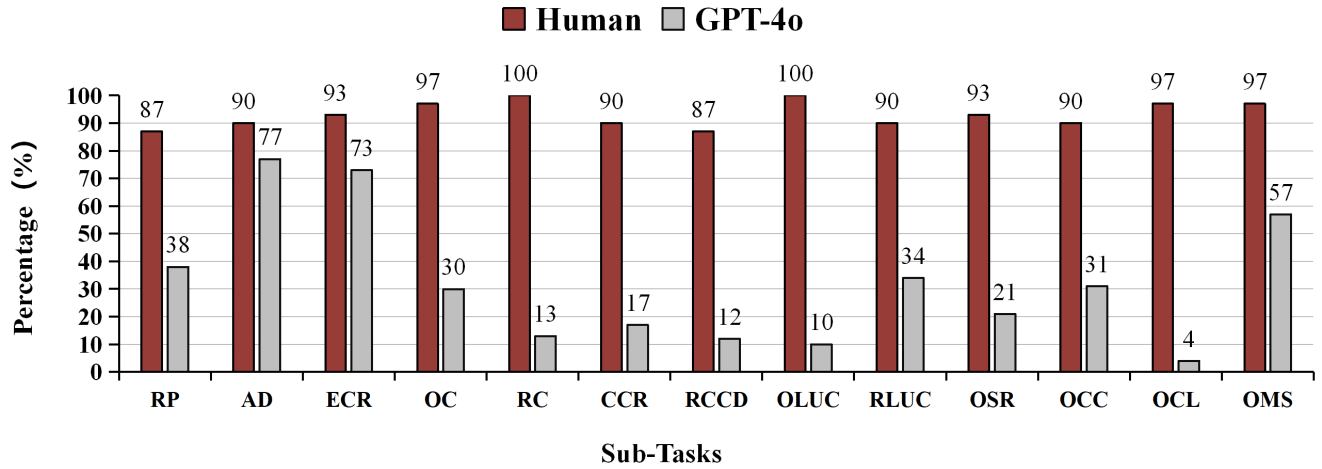


Figure 5. Evaluation results of XLRs-Bench and MLLMs. “RP”, “AD”, “ECR”, “OCC”, “RC”, “CCR”, “RCCD”, “OLUC”, “RLUC”, “OSR”, “OCC”, “OCL”, and “OMS” each indicate a specific task domain: Route Planning, Anomaly Detection, Environmental Conditional Reasoning, Overall Counting, Regional Counting, Counting with Complex Reasoning, Regional Counting with Change Detection, Overall Land Use Classification, Regional Land Use Classification, Object Spatial Relationship, Object Classification, Object Color and Object Motion State.

tings, underscoring the need for more effective multimodal representation learning. Future research could focus on better visual feature extraction, enhanced language alignment, and stronger generalization and reasoning in complex, high-resolution contexts.

A.5. Sub-tasks (L-3 capability) Results on XLRs-Bench

This section highlights the performance of MLLMs across all L-3 capabilities. The VQA task is split into perception and reasoning dimensions, with results shown in Tables 6 and 7, respectively. L-3 capabilities for the Visual Ground-

Table 6. **Experimental results of L-3 capability on the perception dimension of VQA tasks.** Models are ranked according to their average performance. Rows corresponding to proprietary models are highlighted in gray for distinction. “OC”, “RC”, “OLUC”, “RLUC”, “OSR”, “OCC”, “OCL” and “OMS” each indicate a specific task domain: Overall counting, Regional Counting, Overall Land Use classification, Regional Land Use Classification, Object Spatial Relationship, Object Classification, Object Color and Object Motion State.

Method	LLM	Language	Perception								
			Subtasks (L-3 Capability)			OC	RC	OLUC	RLUC	OSR	OCC
CogVLM2	Llama3-8B	en	31.89	38.48	1.53	68.07	35.92	40.77	30.93	64.53	37.65
LLaVA-OneVision	Qwen2-7B	en	29.19	38.37	1.11	70.50	32.60	35.63	34.37	62.50	36.54
Qwen2-VL	Qwen2-7B	en	32.43	42.49	5.86	68.99	32.04	35.05	33.34	59.53	36.09
GPT-4o-mini	-	en	20.27	31.38	18.69	58.52	29.96	39.97	30.56	63.44	35.71
InternVL2	InternLM2.5-7B	en	22.97	38.07	8.19	62.84	26.60	35.02	32.79	60.94	34.37
InternLM-XComposer-2.5	InternLM2-7B	en	26.76	39.30	1.11	70.01	32.75	33.41	29.06	11.72	32.90
LLaVA-Next	Llama3-8B	en	27.84	41.87	1.11	60.14	32.50	29.60	30.59	63.12	32.72
GPT-4o	-	en	24.32	31.48	16.81	64.02	32.35	19.59	29.00	40.31	28.70
LLaVA-1.5	Vicuna-7B	en	24.05	22.12	0.00	29.29	23.05	21.65	17.45	38.12	20.77
GeoChat	Vicuna-7B	en	24.05	22.12	1.00	27.72	23.30	21.65	17.45	38.13	20.74
Qwen2-VL	Qwen2-7B	zh	32.16	42.28	1.77	72.44	33.26	40.07	34.06	60.00	38.29
InternVL2	InternLM2.5-7B	zh	22.43	38.99	3.65	56.42	34.24	39.60	33.75	60.78	36.97
LLaVA-OneVision	Qwen2-7B	zh	27.03	41.46	1.11	69.47	31.73	39.00	28.33	62.50	35.56
GPT-4o-mini	-	zh	20.00	33.13	25.66	53.13	29.59	37.58	31.18	63.28	34.98
InternLM-XComposer-2.5	InternLM2-7B	zh	23.24	43.21	1.22	63.59	32.62	33.92	31.55	51.72	34.44
CogVLM2	Llama3-8B	zh	27.84	39.40	11.50	62.51	34.57	29.26	30.56	62.81	33.37
LLaVA-Next	Llama3-8B	zh	29.73	34.36	1.33	58.14	31.98	26.58	29.85	61.88	31.00
GPT-4o	-	zh	18.11	23.87	12.39	61.60	31.25	13.91	33.57	62.19	27.95
GeoChat	Vicuna-7B	zh	24.05	22.12	0.72	28.16	23.05	21.65	17.45	38.13	20.72
LLaVA-1.5	Vicuna-7B	zh	24.05	22.12	0.66	28.05	23.01	21.65	17.45	38.12	20.70

ing task are summarized in Table 8.

MLLMs generally excel in reasoning tasks compared to perception tasks in XLRs-Bench. On most benchmarks [34, 77], MLLMs excel in perception tasks but struggle with reasoning, which requires complex conditional interpretation. However, XLRs-Bench presents a reversed trend: MLLMs perform worse in perception due to its ultra-high-resolution images averaging $8,500 \times 8,500$ pixels—24 times higher than those in MME-Realworld [77]. With a 4K resolution limit, current MLLMs cannot process such detailed imagery effectively. In contrast, reasoning tasks, often based on global patterns, are less resolution-dependent. XLRs-Bench highlights the need for next-generation MLLMs capable of handling ultra-high-resolution data, a crucial step for real-world remote sensing applications.

Capturing local features is crucial for perception tasks. Ultra-high-resolution visual tasks like Object Spatial Relationship (OSR) and Object Color (OCL), as shown in Tables 6-8, exhibit significantly lower accuracy. For example, LLaVA1.5 achieves only 17.45% on the OCL task in the Chinese benchmark. This shortfall arises from three main factors: 1. Limited sensitivity to sparse details. Ultra-high-resolution images (e.g., $8,500 \times 8,500$ pixels) feature sparse yet critical details, such as small object contours and intricate local relationships. Existing MLLMs, optimized for global feature extraction, struggle to detect these fine-grained signals, impairing performance on detail-oriented

tasks. 2. Imbalanced global and local feature modeling. Current visual encoders emphasize global semantics over local-global interactions. For instance, OCL tasks require identifying subtle color variations among objects in localized regions, yet an overemphasis on global features can lead to misclassification of these local color details. 3. Resolution and computational constraints. MLLMs face input resolution limits (e.g., 4K), necessitating downsampling that degrades local features and hampers detailed modeling. Ultra-high-resolution scenarios demand enhanced local feature modeling to meet their complex requirements. Strengthening this capability is essential for improving performance in these perception tasks.

A.6. Samples and Hard Cases of XLRs-Bench

In this section, we present examples of the VQA (Fig. 6), image captioning (Fig. 8 and Fig. 9), and visual grounding tasks (Fig. 7). What’s more, we construct a detailed table (Tab. 9) analyzing model performance and error causes for each L-3 subtask. We then use examples to thoroughly illustrate the errors for each subtask.

In this section, we present a case study analysis of the error types made by LLaVa-Next, Qwen2-VL, and LLaVA-OneVision on various sub-tasks in XLRs-Bench. We classify the errors into the following 5 categories, following the MMT-Bench [67]:

Perception Error: MLLMs often struggle to recognize, classify, or detect objects and content in images,

Table 7. **Experimental results of L-3 capability on the reasoning dimension of VQA tasks.** Models are ranked according to their average performance. Rows corresponding to proprietary models are highlighted in gray for distinction. “RP”, “AD”, “ECR”, “CCR” and “RCCD” each indicate a specific task domain: Route Planning, Anomaly Detection, Environmental Conditional Reasoning, Counting with Complex Reasoning and Regional Counting with Change Detection.

Method	LLM	Language	Reasoning					
			Subtasks (L-3 Capability)			RP	AD	ECR
InternVL2	InternLM2.5-7B	en	33.01	74.54	77.07	54.12	44.44	58.97
InternLM-XComposer-2.5	InternLM2-7B	en	35.31	69.50	77.87	49.59	32.22	56.83
Qwen2-VL	Qwen2-7B	en	32.12	68.35	79.29	46.81	45.93	56.33
LLaVA-Next	Llama3-8B	en	26.02	69.10	76.00	45.47	32.22	53.14
LLaVA-OneVision	Qwen2-7B	en	24.07	71.88	79.91	37.76	37.78	53.00
GPT-4o	-	en	41.24	72.06	75.29	26.34	21.85	52.79
CogVLM2	Llama3-8B	en	34.16	69.85	73.07	45.37	-	52.70
GPT-4o-mini	-	en	33.81	72.06	75.02	31.49	15.19	51.60
LLaVA-1.5	Vicuna-7B	en	38.67	34.70	41.51	25.00	29.26	34.97
GeoChat	Vicuna-7B	en	32.12	33.25	34.84	25.10	-	29.71
InternVL2	InternLM2.5-7B	zh	40.09	76.57	85.51	48.97	44.07	62.14
Qwen2-VL	Qwen2-7B	zh	24.34	76.57	83.11	49.69	44.44	57.89
LLaVA-OneVision	Qwen2-7B	zh	29.12	74.80	82.13	39.92	30.37	55.51
GPT-4o-mini	-	zh	41.86	74.71	73.78	34.05	21.85	54.84
InternLM-XComposer-2.5	InternLM2-7B	zh	29.47	69.14	80.89	42.28	24.44	54.06
CogVLM2	Llama3-8B	zh	26.19	70.47	75.47	41.15	-	50.60
LLaVA-Next	Llama3-8B	zh	21.59	69.85	73.51	31.58	25.56	48.33
GPT-4o	-	zh	27.08	69.41	66.76	20.78	15.19	45.05
LLaVA-1.5	Vicuna-7B	zh	38.67	37.58	41.60	25.10	29.26	35.72
GeoChat	Vicuna-7B	zh	22.79	23.74	24.44	25.10	-	22.58

Table 8. Visual grounding performance of L-3 capability on XLRs-Bench.

L-3 Capability	Language	Method	GPT-4o	GPT-4o-mini	Qwen2-VL	LLaVA-OneVision	LLaVA-Next	LLaVA-1.5	CogVLM2	InternLM-XComposer-2.5	InternVL2	GeoChat
Fine-grained	en	Acc@0.5	0.70	0.17	0.21	0.25	0.16	0.11	0.02	0.03	0.46	0.21
Visual Grounding		Acc@0.7	0.10	0.06	0.03	0.00	0.08	0.00	0.00	0.02	0.17	0.02
Condition-based	en	Acc@0.5	0.21	0.00	0.08	0.06	0.19	0.06	0.00	0.00	0.19	0.06
Visual Grounding		Acc@0.7	0.00	0.00	0.02	0.00	0.00	0.00	0.00	0.00	0.06	0.00
Fine-grained	zh	Acc@0.5	0.76	0.22	0.22	0.24	0.05	0.13	0.02	0.08	0.38	0.21
Visual Grounding		Acc@0.7	0.05	0.05	0.02	0.02	0.00	0.02	0.00	0.00	0.11	0.02
Condition-based	zh	Acc@0.5	0.14	0.20	0.06	0.02	0.08	0.11	0.03	0.03	0.17	0.06
Visual Grounding		Acc@0.7	0.00	0.00	0.00	0.00	0.03	0.02	0.00	0.00	0.03	0.00

largely due to the limited representational power of their visual encoders, making this the most prevalent error. This perceptual limitation is especially evident in ultra-high-resolution images, where MLLMs often struggle to detect objects with minimal pixel representation. See examples in Fig. 21, Fig. 22, etc.

Reasoning Error : MLLMs accurately perceive visual content but fail in reasoning, resulting in incorrect answers.. See examples in Fig. 10, Fig. 11, etc.

Lack of Knowledge : MLLMs lack the domain-specific knowledge needed to answer specialized questions, such as identifying ship wake information in remote sensing images (see Fig. 21).

Lack of Capability : MLLMs do not have the capability to solve the corresponding tasks. See examples in

Fig. 10, Fig. 12.

Fail to Follow Instruct : MLLMs often misinterpret instructions, leading to errors. For instance, they may misunderstand specific conditions (see Fig. 13) or disregard the instructions entirely, generating errors for the image instead (see Fig. 15).

Overall Land Use Classification

"Q": Select some that best represent the types of land use in the picture. Make sure to include all types present in the image.

A: Crop field **B: Interchange**
C: Multi-unit residential building **D: Shopping center**

Recognition Land Use Classification

"Q": Select the land type for the area circled in red in the image.

"A": Multi-unit residential building
"B": Unit residential building
"C": Educational institution
"D": Impoverished residential area

Anomaly Detection

"Q": Is there a drought or fire phenomenon in any part of the picture?

"A": No
"B": Yes

Object Classification

"Q": Identify the object category within a given reference bounding box from satellite and aerial imagery. bounding box:[546, 63, 632, 146]

"A" White Parking Lot **"B" Green Grassland**
"C" Off-White Roof **"D" Orange Roof**

Object Color

"Q": Determine the color of an object based on a given reference boundary box. bounding box:[42,5045,137,5128]

"A": Blue **"B": Green**
"C": Red **"D": Yellow**

Object Motion State

"Q": Determine whether an object is in motion based on a given reference bounding box. bounding box:[970, 9338, 1127, 9495]

"A": Yes **"B": No**

Object Spatial Relationship

"Q": Which direction is the blue-roofed house surrounded by trees from the nearest gray-roofed house?

"A": upper right **"B": upper left**
"C": right **"D": lower right**

Environmental Condition Reasoning

"Q": Is this region in the picture suitable for wheat cultivation?

(A) The surrounding environment may be affected by industrial pollution or pesticide residues, making it unsuitable for growing food crops.
(B) The success of agriculture in a region depends not only on natural conditions but also on market and economic factors. If the local area lacks sales channels, has inadequate processing capacity, or farmers cannot obtain reasonable prices, then even fertile land may not be suitable for commercial cultivation.
(C) It is suitable for cultivation. This area is divided into many small fields with varying shades of color, which may represent different crop types or growth stages. This land use pattern usually implies precise agricultural management, which is conducive to crop rotation and the rational use of land resources.
(D) Although most of the area looks lush and green, there are also some brown patches, which may be due to seasonal changes.

Route Planning

"Q": What is the best route from the housing cluster in the top right corner of the picture to the river bifurcation below?

(A) Move upwards, then slightly to the right, following the river bifurcation .
(B) Move directly upwards, follow the river.
(C) Move upwards, then slightly to the left, following the river bifurcation .
(D) Move upwards, then slightly to the right, avoiding the main road.

Counting with Complex Reasoning

"Q": How many ponds or lakes are there on the left side of the picture?

"A": Four **"B": Six**
"C": Five **"D": Seven**

Overall Counting

"Q": How many vehicles are there in the entire picture?

"A": Fifty-one **"B": Fifty-two**
"C": Sixty-one **"D": Sixty-two**

Regional Counting

"Q": How many orange roofs are there within the red circle?

"A": Three **"B": Four**
"C": Five **"D": Six**

Fine-grained Visual Grounding

"Q": Three houses are grouped together, resembling a courtyard house ,with a row of trees beneath them. In the top left corner, there is a circular tree. [7942,8617,8105,8762]

Condition-based Visual Grounding

"Q": The blue-roofed house and the orange-roofed house surrounded by forest in the bottom right corner of the picture <9890> <9642> <9998> <9810>

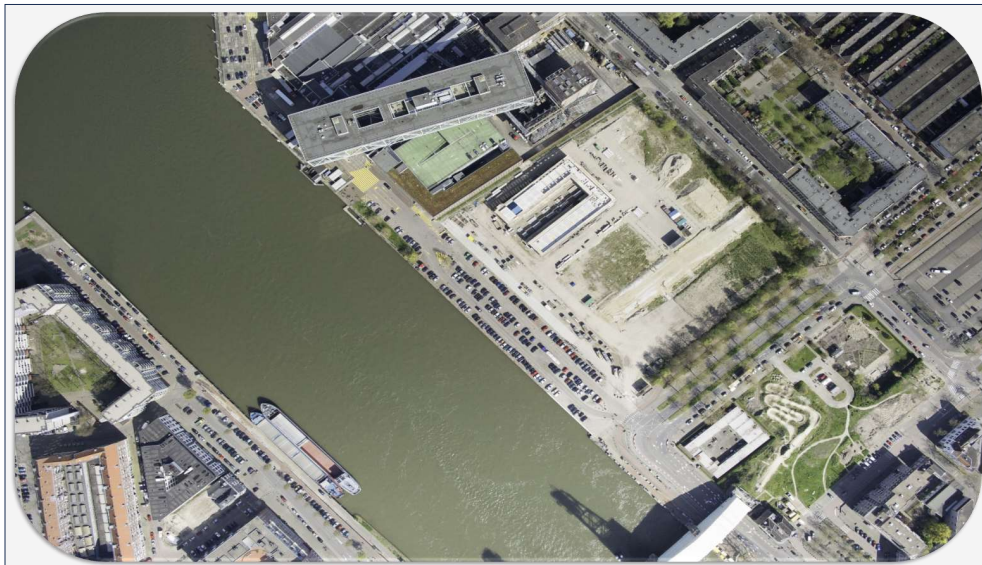
Figure 6. Example of XLRB-Bench in English. XLRB-Bench focuses on large-size ultra-high-resolution remote sensing imagery, integrating over 10 multimodal perception and reasoning tasks within the same image.



Figure 7. **Visual Grounding Results of XLRS-Bench.** Question: "The multi-sided building in the left central area of the picture." The "multi-sided building" required in the ground truth is relatively small and therefore difficult to identify. The GPT-4o model incorrectly classified a similarly shaped roundabout as a polygonal building, while GeoChat [23] misidentified an irregularly shaped parking lot as a polygonal building.



Figure 8. **Image Captioning Results of XLRs-Bench in English.** LLaVA-OneVision and LLaVA-Next face challenges in capturing image details, particularly in conveying critical information like lane counts and vehicle types. Their descriptions often lack depth, failing to convey the richness and nuances of the images. The language is overly rigid and mechanical, struggling to naturally align with the images' context and overall environment.



Ground truth

这张遥感图像展示了一个城市区域，包含河流、建筑群、道路、停车场和绿地。图像从左至右、从上至下被分为九个部分，每个部分展示了城市的不同功能和特征。

1. 在图像的左上部分，显示了一条河流和河岸边的停车场及建筑物。河流呈深灰绿色，沿着图像的中部水平延伸。停车场内停有约**40辆车**，颜色包括白色、黑色、灰色和红色。建筑物的屋顶为灰白色，形状为矩形。
 2. 中上部分展示了一个带有太阳能板的长条形建筑，下方停有多辆主要为黄色和白色的车辆，右侧开放停车场中车辆主要为黑色、白色和灰色。
 3. 右上部分是一条河流旁的道路，上有多辆车辆行驶，道路呈直线形状，宽度均匀。河中有一艘大型游船，船身为白色。
 4. 左中部分显示了一个城市交叉口，包括多条道路、车辆和树木。交叉口中有车辆，颜色包括蓝色、白色、黑色和红色。
 5. 中间部分是一个复杂的建筑群，包括居住和休闲设施，周围环境由道路和少量绿地组成。
 6. 右中部分展示了一个城市河岸景观，包括河流、停车场、直道路和建筑群。停车场内约有**100辆车**，建筑物屋顶为灰色和白色。
 7. 左下部分描述了一个靠近水体的建筑区域，包括建筑、停车场和道路。停车场内约有几十辆车，车辆颜色多样。
 8. 中下部分是一个城市区域，包括建筑物、道路、绿地和停车场。左下角和右下角的停车场内分别停有**15辆**和**12辆车**。
 9. 右下部分展示了一条宽阔的河流和沿河道路，道路上有约**10辆车**行驶，车辆颜色多样。
- 通过这些描述，可以推理出图像展示了一个城市的多功能区域，包括商业、居住和休闲设施。河流和道路的存在表明该城市可能依水而建，且交通发达。**建筑物的密集程度和停车场的充足表明这是一个人口密集且经济活跃的区域。**

LLaVA-OneVision

图像展示了一个城市河岸区域，包括建筑物、道路、绿地和水体。主要元素包括多层建筑、停车场、河流和一些绿色植被。分区描述：

1. 左上角：多层建筑，屋顶为灰色，周围有停车场，车辆颜色多样。（Lack of regional counting）
2. 中上部分：河流沿岸，河岸上有绿色植被和一些小型建筑。
3. 右上部分：道路平行于河流，车辆沿着道路行驶。
4. 左中部分：河流对岸，有更多建筑和停车场。
5. 中间部分：河流中央有一艘船只，河岸两侧有绿色植被。（Lack of regional counting）
6. 右中部分：道路与河流平行，车辆沿着道路行驶。
7. 左下部分：多层建筑，屋顶为红色，周围有停车场。
8. 中下部分：河流沿岸，河岸上有绿色植被和一些小型建筑。（Lack of regional counting）
9. 右下部分：道路与河流平行，车辆沿着道路行驶。（Lack of regional counting）

综合推理：- 功能分区描述：图像显示了工业区（左侧多层建筑）、住宅区（右侧多层建筑）和绿地（河流沿岸的绿色植被）。- 交通网络描述：主要道路平行于河流，车辆沿着道路行驶，形成了城市的交通网络。- 生态与人类活动：河流和绿地提供了生态功能，而多层建筑和停车场则表明这是一个居住和商业混合的区域。河流中央的船只可能用于运输或休闲活动。- 常见物体计数：在图像中可以看到数十辆汽车沿着道路行驶，以及河岸边的几艘船只。（Lack of reasoning to summarize the content of the entire image）

LLaVA-Next

这张遥感图像展示了一个城市的部分区域，主要包括水域、道路、建筑物、绿地和一些交通工具。图像的视角是从高空拍摄的，提供了一个鸟瞰的视野。

1. 从左到右，第一部分显示了一个水域，水面平静，水域的颜色呈现出一种绿色。（Lack of regional counting）
2. 第二部分显示了一个道路，道路呈现出一种灰色，道路的形状是直线，宽度较宽，长度较长，方向是从左到右。
3. 第三部分显示了一个建筑物，建筑物呈现出一种灰色，建筑物的形状是矩形，大小较大，位置在水域的右侧。
4. 第四部分显示了一个绿地，绿地呈现出一种绿色，绿地的形状是长方形，大小较大，位置在建筑物的右侧。
5. 第五部分显示了一个建筑物，建筑物呈现出一种灰色，建筑物的形状是矩形，大小较大，位置在绿地的右侧。（Lack of regional counting）
6. 第六部分显示了一个道路，道路呈现出一种灰色，道路的形状是曲线，宽度较宽，长度较长，方向是从左到右。
7. 第七部分显示了一个建筑物，建筑物呈现出一种灰色，建筑物的形状是矩形，大小较大，位置在道路的右侧。
8. 第八部分显示了一个绿地，绿地呈现出一种绿色，绿地的形状是长方形，大小较大，位置在建筑物的右侧。（Lack of regional counting）
9. 第九部分显示了一个建筑物，建筑物呈现出一种灰色，建筑物的形状是矩形，大小较大，位置在绿地的右侧。（Lack of regional counting）

整体上，这张遥感图像展示了一个城市的部分区域，主要包括水域、道路、建筑物、绿地和一些交通工具。交通工具包括了一个船只和一些车辆。道路布局呈现出一种复杂的交通网络，包括直线和曲线的道路。建筑物的密度较高，包括了各种功能类型。绿地的分布较均匀，包括了草地和树木。水域的颜色呈现出一种绿色，表明水域的水质较好。这张图像提供了一个城市的鸟瞰视野，展示了城市的交通、建筑和生态等方面的信息。（Lack of reasoning to summarize the content of the entire image）

Figure 9. Image Captioning Results of XLRs-Bench in Chinese. Both LLaVA-Next and LLaVA-OneVision share a key weakness: the inability to perform local counting. LLaVA-Next shows notable limitations and a narrow focus when describing localized features, resulting in overly simplistic outputs. While LLaVA-OneVision offers greater diversity and detail, it still lacks sufficient complexity. More importantly, both models are confined to directly describing objects in images without engaging in deeper reasoning or analysis, restricting their practical utility.

Table 9. Table index of case study figures by sub-tasks (L-3 capability) with associated (error) categories for each MLLM.

Case Figure	L-2 task	L-3 task	LLaVa-Next	Qwen2-VL	LLaVA-OneVision
Fig. 10	Anomaly detection	Anomaly detection and interpretation	Lack of Capability	Reasoning Error	Lack of Capability
Fig. 11	Complex reasoning	Environmental condition reasoning	Reasoning Error	Correct	Correct
Fig. 12	Planning	Route planning	Lack of Capability	Lack of Capability	Lack of Capability
Fig. 13	Spatiotemporal reasoning	Counting with change detection	Lack of Capability	Fail to Follow Instruct	Lack of Capability
Fig. 14	Complex reasoning	Counting with complex reasoning	Lack of Capability	Fail to Follow Instruct	Correct
Fig. 15	Counting	Overall counting	Lack of Capability	Lack of Capability	Lack of Capability
Fig. 16	Counting	Regional counting	Lack of Capability	Lack of Capability	Lack of Capability
Fig. 17	Scene classification	Overall land use classification	Perception Error	Correct	Perception Error
Fig. 18	Scene classification	Regional land use classification	Perception Error	Correct	Correct
Fig. 19	Object properties	Object classification	Correct	Correct	Lack of Capability
Fig. 20	Object properties	Object color	Correct	Perception Error	Perception Error
Fig. 21	Object properties	Object motion state	Perception Error	Lack of Knowledge	Lack of Knowledge
Fig. 22	Object spatial relationship	Object spatial relationship	Perception Error	Perception Error	Correct

Anomaly detection and interpretation

Question: Why are there many industrial areas clustered together on the left side of the highway in the lower left of the picture?

Options

- (A) Because the region is close to railways or airports, it facilitates the transportation of raw materials and finished products.',
- (B) The region has abundant natural resources, such as coal and iron, suitable for the development of heavy industry.',
- (C) This layout may be the result of urban planning, aimed at separating industrial activities from agricultural production areas to reduce environmental impact.',
- (D) The regional government has offered preferential policies, attracting a large number of enterprises to invest in building factories.

Answer: C

10000×10000



 Lack of Capability

LLaVA-Next:A

The correct answer is (A) Because the region is close to railways or airports, it facilitates the transportation of raw materials and finished products. The image shows a landscape with a highway running through it, and on the left side of the highway, there are many industrial areas clustered together. This layout is likely due to the presence of transportation infrastructure such as railways or airports nearby. These transportation networks make it easier and more cost-effective to move raw materials and finished products, which is essential for the operation of industrial facilities. The concentration of industrial areas in this region suggests that the transportation infrastructure plays a significant role in the development and growth of the industrial sector in this area.

 Reasoning Error

Qwen2-VL:D

The correct answer is (D) The regional government has offered preferential policies, attracting a large number of enterprises to invest in building factories. The image shows a mix of agricultural fields and industrial areas. The clustering of industrial areas on the left side of the highway in the lower left of the picture suggests a deliberate layout. This type of arrangement is often seen in regions where the government has implemented policies to attract industries. Preferential policies can include tax incentives, land allocation, and infrastructure development, which make the area more attractive for businesses. This strategic placement helps in the economic development of the region by creating jobs and promoting industrial growth.

 Lack of Capability

LLaVA-OneVision: A

The clustering of industrial areas near the highway suggests a strategic location that facilitates transportation. Proximity to major transport routes like highways often enhances the efficiency of moving raw materials and finished products, making option (A) the most plausible explanation.

Figure 10. A sample case of Anomaly detection and interpretation.

Environmental condition reasoning

Question: According to satellite images, the area covered by greenery and land is extensive and evenly distributed, yet the residential areas are very dense. Why does this phenomenon occur?

10000×10000



Options

- (A) This layout may be due to the fact that the region has historically been an agricultural area, thus preserving a large amount of farmland and green spaces. Over time, as urbanization has accelerated, the original agricultural land has been retained, forming the current landscape.
- (B) The planners of the region may believe that dispersed residential areas and concentrated green spaces can create a harmonious living environment, bringing people closer to nature and allowing them to enjoy a tranquil lifestyle.
- (C) Concentrated residential areas are likely located near transportation hubs or business centers, facilitating residents' travel and work, while also providing the necessary space for urban development.
- (D) This layout may be intended to protect the natural environment and ecological balance, while also meeting human residential needs. Large areas of green space can provide more ecosystem services, such as air purification and water conservation, while concentrated residential development can enhance land use efficiency and reduce the impact on the surrounding environment.

Answer: D



Reasoning Error

LLaVA-Next: A

The correct answer is (A) This layout may be due to the fact that the region has historically been an agricultural area, thus preserving a large amount of farmland and green spaces. Over time, as urbanization has accelerated, the original agricultural land has been retained, forming the current landscape.



Qwen2-VL: D

The correct answer is (D). The image shows a mix of agricultural land, green spaces, and residential areas. The extensive greenery and land patches suggest that the region has historically been agricultural, which has been preserved over time. The dense residential areas indicate that urbanization has occurred, but the green spaces have been maintained, forming a harmonious landscape.



LLaVA-OneVision: D

The image shows a landscape where there are extensive areas of greenery and land, but also densely populated residential areas. This phenomenon can be attributed to several factors: Historical Context: The region may have historically been an agricultural area, with large tracts of land dedicated to farming. Over time, as urbanization accelerated, the original agricultural land was retained, forming the current landscape. This is evident in the large patches of green fields that are interspersed with residential areas.

Figure 11. A sample case of Environmental condition reasoning.

Route planning

Question: What is the shortest route from the triangular road above the largest cluster of houses in the top right corner of the picture to the nearest roundabout below it to the left?

Options

- (A) Starting from the intersection at the upper left of the triangular road, head south along the road, turn right at the fourth intersection, continue west, turn left at the third intersection, proceed to the end of the road, turn left, and continue for a while to reach your destination.'
- (B) Starting from the intersection at the upper left of the triangular road, head south along the road, turn right at the fourth intersection, continue west, turn left at the third intersection, proceed to the end of the road, turn right, and continue straight for a while to reach your destination.'
- (C) Starting from the intersection at the upper left of the triangular road, head south along the road, turn left at the first intersection, continue along the road, turn left at the next intersection, and proceed for a while to reach your destination.'
- (D) Starting from the intersection at the upper left of the triangular road, head south along the road, pass four intersections, and continue for a while to reach your destination.

Answer: D

10000×10000



 Lack of Capability

LLaVA-Next:A

The shortest route from the triangular road above the largest cluster of houses in the top right corner of the picture to the nearest roundabout below it to the left is option (A). Starting from the intersection at the upper left of the triangular road, you head south along the road. At the fourth intersection, you turn right. Continuing west, you turn left at the third intersection. Proceeding to the end of the road, you turn left, and continue for a while to reach your destination. This route avoids unnecessary turns and takes the most direct path to the roundabout.

 Lack of Capability

Qwen2-VL:B

The shortest route from the triangular road above the largest cluster of houses in the top right corner of the picture to the nearest roundabout below it to the left is (B). Starting from the intersection at the upper left of the triangular road, head south along the road, turn right at the fourth intersection, continue west, turn left at the third intersection, proceed to the end of the road, turn right, and continue straight for a while to reach your destination.

 Lack of Capability

LLaVA-OneVision: B

The shortest route from the triangular road above the largest cluster of houses in the top right corner of the picture to the nearest roundabout below it to the left would be option B. This route involves traveling south along the road, passing four intersections, and continuing for a while until reaching the roundabout.

Figure 12. A sample case of Route planning.

Counting with changing detection

10000×10000

Question: How many changes are there in the number of houses within the red-circled areas corresponding to the two pictures?

Options

- (A) 4
- (B) 3
- (C) 6
- (D) 5

Answer: D



Lack of Capability

LLaVA-Next: B

The correct answer is (B) .To explain, let's analyze the red-circled areas in the two images: 1. In the top image, there are three distinct areas with houses within the red circles. 2. In the bottom image, there are also three distinct areas with houses within the red circles. The number of houses within the red-circled areas remains consistent across the two images, which is why the correct answer is (B) 3.



Fail to Follow Instruct

Qwen2-VL: B

The correct answer is (B) 3. To determine the number of changes in the number of houses within the red-circled areas corresponding to the two pictures, we need to compare the houses in each area in both images.\n\n1. **First Image:**\n - Red-circled area 1: 2 houses\n - Red-circled area 2: 3 houses\n - Red-circled area 3: 1 house\n - Red-circled area 4: 2 houses\n\n2. **Second Image:**\n - Red-circled area 1: 3 houses\n - Red-circled area 2: 4 houses\n - Red-circled area 3: 2 houses\n - Red-circled area 4: 3 houses



Lack of Capability

LLaVA-OneVision: B

The answer is B.

Figure 13. A sample case of Counting with change detection.

Counting with complex reasoning

4912x7360

Question: How many cars are on the road in the downward direction from the intersection in the upper right corner of the picture??

Options

- (A) 7
- (B) 6
- (C) 4
- (D) 5

Answer: B



 Lack of Capability

LLaVA-Next:C

The correct answer is (C). To count the number of cars on the road in the downward direction from the intersection in the upper right corner of the picture, we need to look at the road that appears to be a one-way street. From the intersection, we can see that the road is clear and there are four cars visible on this road. The cars are aligned in a straight line, indicating that they are moving in the same direction. The cars are not overlapping, so we can count them accurately. The other roads in the image are not in the downward direction from the intersection, so they do not contribute to the count.

 Lack of Capability

Qwen2-VL:C

The correct answer is (C). In the image, there is an intersection in the upper right corner. From this intersection, the road goes downward in a straight line. Counting the cars on this road, there are exactly 4 cars visible.

 Lack of Capability

LLaVA-OneVision: A

There are 7 cars on the road in the downward direction from the intersection in the upper right corner of the picture.

Figure 14. A sample case of Counting with complex reasoning.

Overall counting

Question: How many cars are there in the whole picture?

Options

(A) 107

(B) 172

(C) 144

(D) 165

Answer: D

6000×6000



Lack of Capability

LLaVA-Next:C

The correct answer is (C) 144. The image shows a large parking lot with multiple rows of cars parked in an orderly manner. To count the number of cars, I would need to know the exact dimensions of the parking lot and the number of cars in each row. However, without that information, I can only provide an estimate based on the visible area. From the image, it appears that there are at least 144 cars visible. The actual number could be higher if there are additional rows of cars not visible in the image or if the cars are packed more tightly than they appear in the photo.



Fail to Follow Instruct

Qwen2-VL:B

The correct answer is (B) 172. To determine the number of cars in the picture, we need to count the cars in each visible parking area and on the roads. Here is the breakdown:
Parking Areas:
- Top right corner: 10 cars
- Top left corner: 5 cars
- Bottom left corner: 10 cars
- Bottom right corner: 15 cars
- Middle left area: 10 cars
- Middle right area: 10 cars
- Middle bottom area: 10 cars
- Middle top area: 10 cars
- Middle bottom right area: 10 cars
- Middle bottom left area: 10 cars
- Middle top left area: 10 cars
- Middle top right area: 10 cars
- Middle bottom center area: 10 cars
- Middle top center area: 10 cars
- Middle bottom center right area: 10 cars



LLaVA-OneVision: D

There are 165 cars in the picture.

Figure 15. A sample case of Overall counting.

Regional counting

4912×7360

Question: How many cars are there inside the red circle?

Options

- (A) 17
- (B) 178
- (C) 19
- (D) 20

Answer: D



Lack of Capability

LLaVA-Next:C

The correct answer is (C). To explain, the image shows an aerial view of a city with various buildings, roads, and parking areas. The red circle is drawn around a specific area within the city. Inside this circle, there are 19 cars visible. The cars are parked along the sides of the roads and in designated parking spaces. The number of cars can be counted by visually identifying each car within the red circle. The other options (A, B, and D) are incorrect because they do not match the number of cars visible in the red circle.



Lack of Capability

Qwen2-VL:A

The correct answer is (A). To determine the number of cars inside the red circle, we need to carefully count each car within the designated area. The red circle is drawn around a specific section of the image, and by examining the area within this circle, we can see a total of 17 cars.



Lack of Capability

LLaVA-OneVision: A

There are 17 cars inside the red circle.

Figure 16. A sample case of Regional counting.

Overall Land use classification

4096x4096

Question: Choose some land use types that best describes the image. Requires all types contained in the picture to be selected.

Options

- (A) Port
- (B) Aquaculture
- (C) Burial Site
- (D) Crop Field

Answer: ABD



Perception Error

LLaVA-Next: ABCD

The image shows a coastal area with various land use types. The correct answer is: (A) Port (B) Aquaculture (C) Burial Site (D) Crop Field. The image shows a coastal area with a body of water, which appears to be a river or a bay. There are several boats visible on the water, indicating that this is a port or a harbor. The presence of a large building with a dome-like structure suggests that there might be a significant industrial or commercial activity in the area. The land is divided into different sections, some of which are likely used for agricultural purposes, as indicated by the rectangular fields. There are also areas that seem to be used for residential purposes, as evidenced by the clusters of buildings. The presence of a road network suggests that this is a developed area with infrastructure. The overall layout and the presence of a large body of water suggest that this is a port or a harbor area. Aquaculture is also a possibility, as there are areas that could be used for fish farming. However, without more specific details, it is not possible to confirm the presence of a burial site. Crop fields are also present, as indicated by the rectangular fields.



Qwen2-VL: ABD

Correct answer: (A) Port, (B) Aquaculture, (D) Crop Field



Perception Error

LLaVA-OneVision: ABCD

The image shows a river with boats, indicating that it is navigable and possibly used for transportation or recreation. There are industrial buildings along the riverbank, suggesting that this area may be used for manufacturing or other industrial activities. The presence of green areas indicates that there are parks or undeveloped land in the vicinity. The grid-like pattern of the land suggests that some parts of the area are used for agriculture, as these are often organized in such patterns for efficient farming practices. Therefore, the correct options are A (Port), B (Aquaculture), D (Crop Field), and potentially C (Burial Site) if there are any cemeteries in the area.

Figure 17. A sample case of Overall land use classification.

Regional Land use classification

10000×10000

Question: Select the land use types in the areas circled in red within the image.

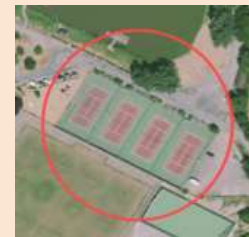


Options

- (A) Golf Course
- (B) Park
- (C) Recreational Facilities
- (D) Stadium



Answer: D



Perception Error

llama3-llava-next-8b: A

The circled areas in the image appear to be well-maintained and have a pattern that is typical of a golf course. Golf courses are designed with a series of holes, each consisting of a tee box, fairway, rough, and putting green, with a flagstick and a hole. The layout and the green spaces suggest that these areas are likely designated for golfing activities. The presence of a body of water nearby also indicates that the golf course might have water hazards, which are common features in golf course designs.



Qwen2-VL: C

The correct answer is (C). The areas circled in red appear to be small, rectangular plots of land with a more uniform and organized appearance compared to the surrounding agricultural fields. This suggests that they are likely to be recreational facilities, such as sports fields, parks, or other types of recreational areas. The uniformity and the presence of what appears to be a small building or structure within these areas further support this classification.



LLaVA-OneVision: C

The land use type in the area circled in red appears to be a recreational facility. This is indicated by the presence of open spaces, pathways, and possibly sports fields or other recreational amenities. The layout suggests it is designed for public use, which aligns with the characteristics of a recreational facility.

Figure 18. A sample case of Regional land use classification.

Object classification

6000×6000

Question: Recognize the category of objects from satellite and aerial images given the bounding boxes for referring objects.
The resolution of satellite image is 6000 x 6000. Bounding box: [2079,3574,2238,3637]

Options

- (A) white van
- (B) blue vehicle
- (C) red truck
- (D) grey buildings

Answer: D



LLaVA-Next: A

The correct answer is (A) white van. The bounding box [2079,3574,2238,3637] is likely a white van due to its size and color. The resolution of the satellite image is 6000 x 6000, which allows for a clear distinction between different types of vehicles. The white van is distinguishable from other vehicles such as the blue vehicle, red truck, and grey buildings. The van's color and shape are more prominent in the image, making it easier to identify. The other bounding boxes are for different types of objects, such as buildings and vehicles, but the one in question is specifically for a white van.



Qwen2-VL: A

The correct answer is (A) white van. The image shows an aerial view of a city area with various buildings, roads, and vehicles. The bounding box [2079,3574,2238,3637] is located on the ground, and within this area, there is a white van parked on the street. The van is clearly visible and identifiable by its white color and shape, making it the correct choice.



Lack of Capability

LLaVA-OneVision: D

The bounding box you provided [2079,3574,2238,3637] corresponds to a small section of the image. Based on the context and the objects visible in that specific area, it appears to be part of a road or pathway. The resolution of 6000 x 6000 suggests that this is a zoomed-in view of a larger area, which includes residential buildings with red roofs, as seen in the surrounding areas. The objects within the bounding box do not seem to match any of the options A, B, C, or D directly. However, since the bounding box is so small and only shows a portion of the image, it's challenging to determine the exact nature of the object without more context. If we were to interpret the bounding box as a single object, it might be considered a "grey building" (D) due to its proximity to the buildings with red roofs, but this is speculative given the limited information available from such a small section of the image.

Figure 19. A sample case of Object classification.

Object color

4912x7360

Question: Determine the color of the object based on the given reference boundary box. The resolution of the satellite image is 7360 x 4912. Bounding box coordinates: [3620, 1651, 3604, 1759].

Options

- (A) Red
- (B) Yellow
- (C) Black
- (D) White

Answer: C



LLaVA-Next: C

The color of the object based on the given reference boundary box is (C) Black. The object in question appears to be a building or a section of a building with a dark roof. The image resolution is 7360 x 4912, which allows for a clear view of the object's color. The bounding box coordinates [3620, 1651, 3604, 1759] indicate the specific area of the image where the object is located. The object's color is consistent with the color of the roof, which is black. The surrounding area includes other buildings, roads, and green spaces, but the object in question is the only one that matches the color (C) Black.



Perception Error

Qwen2-VL:A

The correct answer is (A) Red. The object in question is located at the coordinates [3620, 1651, 3604, 1759] in the satellite image. Based on the color and shape of the object, it appears to be a tennis court, which is typically colored red. The surrounding area includes buildings and streets, which are not the focus of this question. Therefore, the correct answer is (A) Red.



Perception Error

LLaVA-OneVision: A

The color of the object in question is red. This can be determined by examining the bounding box coordinates provided, which are [3620, 1651, 3604, 1759]. By looking at the image and focusing on the area defined by these coordinates, it becomes clear that the object has a distinct red color. The surrounding objects have different colors, such as white, gray, and blue, but the object in question stands out due to its red hue.

Figure 20. A sample case of Object color.


Object motion state

Question: Determine the motion state of an object based on the given reference bounding box. The resolution of the satellite image is 10000 x 10000. Bounding box coordinates: [7846, 428, 7862, 440].

Options
 (A) Yes
 (B) No

Answer: A

10000x10000



Perception Error

LLaVA-Next:B

The reference bounding box coordinates you provided are very small and do not correspond to any significant object in the image. The image appears to be a satellite view of a landscape with fields, roads, and possibly a body of water. The bounding box you provided is too small to be discernible or to determine the motion state of an object. To determine the motion state of an object, one would typically look for changes in position, orientation, or size over time, which are not apparent from the given bounding box coordinates.

Lack of Knowledge

Qwen2-VL:B

The given reference bounding box coordinates [7846, 428, 7862, 440] are within the image, but the object within this bounding box appears to be a small, isolated patch of land or water. There is no clear indication of motion, such as a moving object or a change in the position of the object over time. Therefore, based on the given image and the reference bounding box, it is not possible to determine the motion state of the object.

Lack of Knowledge

LLaVA-OneVision: B

The bounding box coordinates provided are [7846, 428, 7862, 440]. These coordinates represent a very small rectangular area within the larger image. Given that the resolution of the satellite image is 10000 x 10000, this bounding box corresponds to a very tiny portion of the entire image. To determine the motion state of an object based on this bounding box, we would need more information about what kind of object we are looking at and how it might move. However, since the bounding box is so small and does not encompass any significant features or objects, it is not possible to accurately determine the motion state of anything within this bounding box. Therefore, the answer to the question "Determine the motion state of an object based on the given reference bounding box" with the bounding box coordinates [7846, 428, 7862, 440] is B) No, because the bounding box is too small to provide any meaningful information about motion.

Figure 21. A sample case of Object motion state.

Object spatial relationship

Question: The upper right corner of the picture is an open area.
In which direction is the tree facing the person

Options

- (A) Upper Right
- (B) Above
- (C) Below
- (D) Lower Left

Answer: D

4912x7360



Perception Error

LLaVA-Next:A

The tree in the image is facing the person in the direction of the upper right corner. This is determined by the orientation of the tree's foliage and the direction of the shadow it casts. The tree appears to be well-lit from the upper right, which suggests that the sun is shining on it from that direction. The shadow of the tree is cast to the left, indicating that the tree is facing towards the upper right corner of the image.



Perception Error

Qwen2-VL:A

The correct answer is (A) Upper Right. The tree in the upper right corner of the picture is facing the person. This can be determined by observing the direction of the tree's branches and leaves, which are oriented towards the upper right part of the image.



LLaVA-OneVision: D

The tree is facing the person in the lower left corner of the image.

Figure 22. A sample case of Object spatial relationship.

A.7. Datasheets

In this section, we document essential details about the proposed datasets and benchmarks following the CVPR Dataset and Benchmark guidelines and the template provided by Gebru *et al.* [14].

A.7.1. Motivation

The questions in this section are primarily intended to encourage dataset creators to clearly articulate their reasons for creating the dataset and to promote transparency about funding interests. The latter may be particularly relevant for datasets created for research purposes.

1. “*For what purpose was the dataset created?*”

A: Existing benchmarks often use significantly smaller image sizes than those found in real-world RS scenarios, have limited annotation quality, and fail to account for key evaluation dimensions. To address these limitations, we introduce XLRs-Bench, a comprehensive benchmark designed to assess the perception and reasoning capabilities of MLLMs in ultra-high-resolution RS contexts.

2. “*Who created the dataset (e.g., which team, research group) and on behalf of which entity?*”

A: The dataset was created by the following authors:

- Fengxiang Wang (National University of Defense Technology)
- Hongzhen Wang (Tsinghua University)
- Mingshuo Chen (Beijing University of Posts and Telecommunications)
- Di Wang (Wuhan University, Zhongguancun Academy)
- Yulin Wang (Tsinghua University)
- Zonghao Guo (Tsinghua University)
- Qiang Ma (Tsinghua University)
- Long Lan (National University of Defense Technology)
- Wenjing Yang (National University of Defense Technology)
- Jing Zhang (Wuhan University)
- Zhiyuan Liu (Tsinghua University)
- Maosong Sun (Tsinghua University)

3. “*Who funded the creation of the dataset?*”

A: The dataset creation was funded by the affiliations of the authors involved in this work.

A.7.2. Composition

Most of the questions in this section are intended to provide dataset consumers with the information they need to make informed decisions about using the dataset for their chosen tasks. Some of the questions are designed to elicit information about compliance with the EU’s General Data Protection Regulation (GDPR) or comparable regulations in other jurisdictions. Questions that apply only to datasets that relate to people are grouped together at the end of the section.

We recommend taking a broad interpretation of whether a dataset relates to people. For example, any dataset containing text that was written by people relates to people.

1. “*What do the instances that comprise our datasets represent (e.g., documents, photos, people, countries)?*”

A: The dataset primarily consists of ultra-high-resolution remote sensing images captured by satellites, along with their corresponding textual annotations. All datasets utilized in XLRs-Bench are publicly accessible and non-profit.

2. “*How many instances are there in total (of each type, if appropriate)?*”

A: XLRs-Bench includes 1,400 ultra-high-resolution images, with 840 reaching a resolution of $10,000 \times 10,000$. Additionally, for these ultra-high-resolution images, we have provided 934 detailed captions, 32,389 VQA pairs, and 12,619 visual grounding instances.

3. “*Does the dataset contain all possible instances or is it a sample (not necessarily random) of instances from a larger set?*”

A: The images in XLRs-Bench are sourced from existing detection [65, 66] and segmentation [6, 10] datasets, but all textual annotations were independently created by us.

4. “*Is there a label or target associated with each instance?*”

A: Yes, for these ultra-high-resolution images, we have provided 934 detailed captions, 32,389 VQA pairs, and 12,619 visual grounding instances.

5. “*Is any information missing from individual instances?*”

A: No, each individual instance is complete.

6. “*Are relationships between individual instances made explicit (e.g., users’ movie ratings, social network links)?*”

A: Yes, the relationship between individual instances is explicit.

7. “*Are there recommended data splits (e.g., training, development/validation, testing)?*”

A: The dataset is designed to evaluate the perception and reasoning abilities of MLLMs, so we recommend using it in its entirety as a test set.

8. “*Is the dataset self-contained, or does it link to or otherwise rely on external resources (e.g., websites, tweets, other datasets)?*”

A: XLRs-Bench is self-contained and will be open-sourced on platforms like Hugging Face, integrated into evaluation tools such as LLMs-Eval [26, 71] for easy use.

9. “*Does the dataset contain data that might be considered confidential (e.g., data that is protected by legal privilege or by doctor–patient confidentiality, data that includes the content of individuals’ non-public communications)?*”

A: No, all data are clearly licensed.

10. “Does the dataset contain data that, if viewed directly, might be offensive, insulting, threatening, or might otherwise cause anxiety?”

A: No, XLRB-Bench does not contain any data with negative information.

A.7.3. Collection Process

In addition to the goals outlined in the previous section, the questions in this section are designed to elicit information that may help researchers and practitioners create alternative datasets with similar characteristics. Again, questions that apply only to datasets that relate to people are grouped together at the end of the section.

1. “How was the data associated with each instance acquired?”

A: The images in XLRB-Bench are sourced from existing detection [65, 66] and segmentation [6, 10] datasets. We enrich these ultra-high-resolution images with manual annotations, including 934 detailed captions, 32,389 VQA pairs, and 12,619 visual grounding instances.

2. “What mechanisms or procedures were used to collect the data (e.g., hardware apparatuses or sensors, manual human curation, software programs, software APIs)?”

A: We employed professional annotation and quality control teams to complete the annotations for VQA and Visual Grounding tasks. For the Image Captioning task, we developed a semi-automated pipeline. Detailed information can be found in Section 3.2 of the main text.

3. “If the dataset is a sample from a larger set, what was the sampling strategy (e.g., deterministic, probabilistic with specific sampling probabilities)?”

A: Please refer to the details listed in the main text Section 3.2.

A.7.4. Preprocessing, Cleaning, and Labeling

The questions in this section are intended to provide dataset consumers with the information they need to determine whether the “raw” data has been processed in ways that are compatible with their chosen tasks. For example, text that has been converted into a “bag-of-words” is not suitable for tasks involving word order.

1. “Was any preprocessing/cleaning/labeling of the data done (e.g., discretization or bucketing, tokenization, part-of-speech tagging, SIFT feature extraction, removal of instances, processing of missing values)?”

A: Yes. During image collection, we prioritized selecting valuable satellite images for annotation. For linguistic annotation, three Level-3 subtasks—Regional Land Use Classification, Regional Counting, and Regional Counting with Change Detection—were marked with red circles. This method, mimicking human interaction, was essential for providing clear, fine-grained region-level analysis on ultra-high-resolution images.

2. “Was the ‘raw’ data saved in addition to the preprocessed/cleaned/labeled data (e.g., to support unanticipated future uses)?”

A: Yes, raw data is accessible.

3. “Is the software that was used to preprocess/clean/label the data available?”

A: Yes, the necessary software used to preprocess and clean the data is publicly available.

A.7.5. Uses

The questions in this section are intended to encourage dataset creators to reflect on tasks for which the dataset should and should not be used. By explicitly highlighting these tasks, dataset creators can help dataset consumers make informed decisions, thereby avoiding potential risks or harms.

1. “Has the dataset been used for any tasks already?”

A: No.

2. “Is there a repository that links to any or all papers or systems that use the dataset?”

A: Yes, we will provide such links in the GitHub and the Huggingface repository.

3. “What (other) tasks could the dataset be used for?”

A: XLRB-Bench provides extensive annotations for VQA, Grounding, and Captioning tasks. In addition to evaluating the perception and reasoning capabilities of existing MLLMs, it can also be used to assess models specifically designed for these tasks.

4. “Is there anything about the composition of the dataset or the way it was collected and preprocessed/cleaned/labeled that might impact future uses?”

A: No.

5. “Are there tasks for which the dataset should not be used?”

A: N/A.

A.7.6. Distribution

Dataset creators should provide answers to these questions prior to distributing the dataset either internally within the entity on behalf of which the dataset was created or externally to third parties.

1. “Will the dataset be distributed to third parties outside of the entity (e.g., company, institution, organization) on behalf of which the dataset was created?”

A: No. The datasets will be made publicly accessible to the research community.

2. “How will the dataset be distributed (e.g., tarball on website, API, GitHub)?”

A: We will provide XLRB-Bench in the GitHub and the Huggingface repository.

3. “When will the dataset be distributed?”

A: We will create a repository to release the data once the paper is officially published, ensuring compliance with the anonymity principle.

4. “Will the dataset be distributed under a copyright or other intellectual property (IP) license, and/or under applicable terms of use (ToU)?”

A: Yes, the dataset will be released under the Creative Commons Attribution-NonCommercial-ShareAlike 4.0 International License.

5. “Have any third parties imposed IP-based or other restrictions on the data associated with the instances?”

A: No.

6. “Do any export controls or other regulatory restrictions apply to the dataset or to individual instances?”

A: No.

A.7.7. Maintenance

As with the questions in the previous section, dataset creators should provide answers to these questions prior to distributing the dataset. The questions in this section are intended to encourage dataset creators to plan for dataset maintenance and communicate this plan to dataset consumers.

1. “Who will be supporting/hosting/maintaining the dataset?”

A: The authors of this work serve to support, host, and maintain the datasets.

2. “How can the owner/curator/manager of the dataset be contacted (e.g., email address)?”

A: The curators can be contacted via the email addresses listed on our paper or webpage.

3. “Is there an erratum?”

A: There is no explicit erratum; updates and known errors will be specified in future versions.

4. “Will the dataset be updated (e.g., to correct labeling errors, add new instances, delete instances)?”

A: Future updates (if any) will be posted on the dataset website.

5. “Will older versions of the dataset continue to be supported/hosted/maintained?”

A: Yes. This initial release will be updated in the future, with older versions replaced as new updates are posted.

6. “If others want to extend/augment/build on/contribute to the dataset, is there a mechanism for them to do so?”

A: Yes, we will provide detailed instructions for future extensions.

A.8. Limitation and Potential Societal Impact

In this section, we discuss the limitations and potential societal impact of this work.

A.8.1. Potential Limitations

While **XLRS-Bench** provides a comprehensive benchmark for evaluating the perception and reasoning capabilities of MLLMs, there are several limitations to consider:

- **Scope of Sensors:** Although our benchmark includes 1,400 ultra-high-resolution visible light remote sensing

images, it may not cover all possible real-world scenarios. There could be additional sensor data, like multispectral data that were not included in this study, potentially limiting the generalizability of our findings.

- **Model and Dataset Diversity:** In this paper, we extensively evaluated both general-purpose and RS-specific MLLMs. As new models emerge, their evaluation results will be added to our open-source leaderboard. Additionally, XLRS-Bench will also be expanded in dataset size and task diversity.

- **Multilingual Support:** XLRS-Bench currently supports both Chinese and English, surpassing the single-language limitations of most remote sensing benchmarks [28]. In the future, we aim to extend support to languages like Spanish and French.

A.8.2. Potential Negative Societal Impact

- **Safety Risks:** XLRS-Bench is designed to evaluate the performance of vision-language multimodal models in ultra-high-resolution remote sensing scenarios. However, excessive reliance on evaluation datasets may lead to overconfidence in autonomous systems, such as multimodal large models. It is crucial to implement adequate safety measures and human supervision when deploying these MLLMs to ensure public safety.

- **Environmental Impact:** Training MLLMs on large datasets and evaluating them using XLRS-Bench requires a certain amount of computational resources. To facilitate future research, we will maintain a leaderboard of MLLMs, removing the need for repeated evaluations of existing models.

- **Bias and Fairness:** XLRS-Bench, with its 16 Level-3 capabilities, is tailored for evaluating ultra-high-resolution remote sensing scenarios. However, it remains limited in comprehensiveness and may exhibit biases. For instance, disaster prediction in anomaly reasoning relies solely on satellite imagery, providing warnings but reflecting inherent biases. Effective decision-making demands the integration of local meteorological and hydrological data. In the future, we aim to expand the evaluation dimensions and datasets to deepen insights into ultra-high-resolution remote sensing applications.